Spatial and Temporal Variability of Sediment Organic Matter Recycling in Two Temperate Eutrophicated Estuaries

Karima Khalil, Mélanie Raimonet, A.M. Laverman, C. Yan, F. Andrieux-Loyer, E. Viollier, B. Deflandre, Olivier Ragueneau, C. Rabouille

Please note that this is an author-produced PDF of an article accepted for publication following peer review. The definitive publisher-authenticated version is available on the publisher Web site

Spatial and Temporal Variability of Sediment Organic Matter Recycling in Two Temperate Eutrophicated Estuaries

Karima Khalil[1, *], Mélanie Raimonet[2], Anniet M. Laverman[2], Chen Yan[2], Françoise Andrieux-Loyer[3], Eric Viollier[4], Bruno Deflandre[5], Olivier Ragueneau[6], Christophe Rabouille[7]

[1] Ecole Supérieure de Technologie d'Essaouira, Université Cadi Ayyad, Km 9, Route d'Agadir, BP. 383, Essaouira, Aljadida, Marocco
[2] UMR 7619 Sisyphe, Université Pierre et Marie Curie/CNRS, 4 place Jussieu, 75252, Paris Cedex 05, France
[3] Département Dyneco Pelagos, Centre de Bres, IFREMER, Plouzané, France
[4] Sorbonne Paris Cité, Institut de Physique du Globe de Paris, UMR 7154 CNRS, Univ. Paris Diderot, 75013, Paris, France
[5] OASU UMR 5805 EPOC, Université de Bordeaux 1, avenue des facultés, 33405, Talence, France
[6] UMR CNRS 6539, Technopôle Brest-Iroise, Institut Universitaire Européen de la Mer, Place Nicolas Copernic, 29280, Plouzané, France
[7] Laboratoire des Sciences du Climat et de l'Environnement, Laboratoire mixte CNRS-CEA, Av. de la Terrasse, 91190, Gif sur Yvette, France

*: Corresponding author : Karima Khalil, email address : ka.khalil@uca.ma

Abstract:

This paper deals with the spatial and seasonal recycling of organic matter in sediments of two temperate small estuaries (Elorn and Aulne, France). The spatio-temporal distribution of oxygen, nutrient and metal concentrations as well as the organic carbon and nitrogen contents in surficial sediments were determined and diffusive oxygen fluxes were calculated. In order to assess the source of organic carbon (OC) in the two estuaries, the isotopic composition of carbon ($\delta^{13}C$) was also measured. The temporal variation of organic matter recycling was studied during four seasons in order to understand the driving forces of sediment mineralization and storage in these temperate estuaries. Low spatial variability of vertical profiles of oxygen, nutrient, and metal concentrations and diffusive oxygen fluxes were monitored at the station scale (within meters of the exact location) and cross-section scale. We observed diffusive oxygen fluxes around 15 mmol m^{-2} day^{-1} in the Elorn estuary and 10 mmol m^{-2} day^{-1} in the Aulne estuary. The outer (marine) stations of the two estuaries displayed similar diffusive O_2 fluxes. Suboxic and anoxic mineralization was large in the sediments from the two estuaries as shown by the rapid removal of very high bottom water concentrations of NO_x^- (>200 µM) and the large NH_4^+ increase at depth at all stations. OC contents and C/N ratios were high in upstream sediments (11–15 % d.w. and 4–6, respectively) and decreased downstream to values around 2 % d.w. and C/N ≤ 10. $\delta^{13}C$ values show that the organic matter has different origins in the two watersheds as exemplified by lower $\delta^{13}C$ values in the Aulne watershed. A high increase of $\delta^{13}C$ and C/N values was visible in the two estuaries from upstream to downstream indicating a progressive mixing of terrestrial with marine organic matter. The Elorn estuary is influenced by human activities in its watershed (urban area, animal farming) which suggest the input of labile organic matter, whereas the Aulne estuary displays larger river primary production which can be either mineralized in the water column or transferred to the lower estuary, thus leaving a lower mineralization in Aulne than

the water column or transferred to the lower estuary, thus leaving a lower mineralization in Aulne than Elorn estuary. This study highlights that (1) meter scale heterogeneity of benthic biogeochemical properties can be low in small and linear macrotidal estuaries, (2) two estuaries that are geographically close can show different pattern of organic matter origin and recycling related to human activities on watersheds, (3) small estuaries can have an important role in recycling and retention of organic matter.

1. Introduction

This paper pays tribute to the vast work of Fred Mackenzie who has been a pioneer and a continuous contributor to the quantification of fluxes between the continent and the ocean. In the spirit of Fred's vision which goes from local investigation of processes to the global scale quantification, this paper deals with local

observations of two specific estuaries on a seasonal basis linked to generalized retention and alteration processes of carbon and nitrogen during its transfer between the continent and the coastal zone.

Estuaries are important filters for both dissolved and particulate components originating from land (Bopp et al. 1982; Nixon et al. 1996; Rabouille et al. 2001; Cloern and Jassby 2012 and references therein), which are ultimately transferred to the coastal sea. A variable proportion of nutrients is consumed by primary production and heterotrophic microbial activity (Cloern 1996), whereas dissolved and particulate carbon is recycled in estuaries (Raymond and Bauer 2001) leading to heterotrophic estuaries representing a net source of CO_2 to the atmosphere (Borges 2005). As a consequence, the organic matter deposited in estuarine sediments originates from autochtonous as well as allochtonous sources (terrestrial, marine) (Cifuentes et al. 1988). Estuarine sediments are important environments regulating carbon, nutrient, metal and sulfur fluxes. The top layers of these sediments are known for their high biogeochemical activity due to organic matter mineralization by a consortium of bacteria using different electron acceptors (oxygen, nitrate, metal oxides, sulfate). Oxygen (O_2) plays an important role in the turnover of organic matter in sediments (Glud 2008) and in the re-oxidation of reduced compounds originating from anoxic mineralization, diffusing up to the oxic zone from deeper layers (Canfield et al. 1993; Deflandre et al. 2002; Pastor et al. 2011a). Denitrification and alternative nitrate removal pathways (Seitzinger 1998; Burgin and Hamilton 2007) that occur in marine and estuarine sediments are also very important in regulating fixed nitrogen fluxes to the coastal zone. Finally, sulfate reduction and methanogenesis are major processes of organic matter degradation in shallow water sediments, which contribute to the overall mineralization of organic carbon and may contribute to the reduction of carbon inputs to the coastal sea (e.g. Middelburg, et al. 1995; Meiggs and Taillefert 2011).

The Elorn and Aulne estuaries are two temperate small estuaries located in Northwestern France. Intense agricultural activity in the watersheds has led to high riverine nitrate inputs, which recurrently lead to green algal blooms downstream of the Elorn Estuary. In spite of these local symptoms, the macrotidal Bay of Brest resists to major eutrophication due to the intense mixing with oceanic waters and to the presence of an invasive benthic filter feeder (Le Pape et al. 1996; Ragueneau et al. 2002; Laruelle et al. 2009). Even if the two estuaries are geographically close, they are characterized by different morphology and by different estuarine and watershed characteristics, which potentially control organic matter quality and recycling together with nutrient fate in the estuary.

The aim of this study is to determine the spatial and temporal variability of carbon, oxygen and nutrient dynamics in sediments of these two small temperate and macrotidal estuaries in order to evaluate the retention

and transformation capacity. The originality of this study is to evaluate the variability of retention and transformation capacity in temperate estuaries that are geographically close, and to link the differences observed with their properties. Therefore, we examined the spatio-temporal distribution of benthic oxygen, pore water nutrients and metals (NO_x^-, NH_4^+, Fe^{2+}, Mn^{2+}, SO_4^{2-} and H_2S) along the salinity gradients during four seasons. In addition, we compared small scale heterogeneity of *in-situ* oxygen microprofiles and porewater profiles to variations at the estuarine scale. Furthermore, the source of the organic carbon in the two estuaries was assessed by its isotopic composition. Finally, we explored the effect of different environmental parameters, such as *in-situ* temperature, salinity, bottom water oxygenation, organic matter input on the organic matter cycling in these estuarine sediments.

2   Materials and methods

2.1 Study sites

The Elorn and Aulne estuaries are located at the interface between the rivers and the semi-enclosed Bay of Brest in Northwestern France (Fig.1). Riverine waters entering these shallow estuaries are particularly rich in nutrients, essentially nitrate, in response to intensive agriculture in the watersheds (Del Amo 1996; Ragueneau et al. 2002). Although the Elorn watershed is 8 times smaller than the Aulne watershed (280 versus 1822 km²), this system is impacted by a higher population (285000 versus 70000 habitants). By its location in Northwerstern France, the whole domain is exposed to an oceanic climate. High precipitation associated to frequent storms are thus observed during winter, which lead to seasonal fluctuations of river discharge from winter (42 and 189 m^3 s^{-1} in 2009) to summer (1.0 and 1.7 m^3 s^{-1} in 2009) in Elorn and Aulne rivers (Banque HYDRO, http://www.hydro.eaufrance.fr). Even if exposed to similar climate by their proximity, the two estuaries differ by their morphology. While the Elorn Estuary is shorter (~ 15 km), straight and more directly exposed to marine hydrodynamic influence, the Aulne estuary is longer (~ 35 km), meandering and more protected by the Bay of Brest.

2.2. Field sampling

Sediment core samples were collected along the Elorn and Aulne estuaries during four cruises in February, May, July and October/November 2009. Sampling was undertaken in the inner (stations E1 and A1), mid (stations E2 and A2) and outer (stations E3 and A3) Elorn and Aulne estuaries (Fig.1). Samples were

119 collected in subtidal shores - between the channel and the border - at mid-tide. Each station was sampled a

120 different day to collect all samples at mid tide. Sediment cores were additionally sampled along the transversal

121 section in the mid Elorn Estuary. The stations (named E2, b, c, d and e) were homogeneously spaced from the

122 left to the right side of the cross-section (75 m width; Fig.1). Sediment cores were sampled from a semi-rigid

123 boat with a gravity corer (UWITEC®) equipped with Plexiglas tubes (8.6-cm internal diameter x 60-cm long).

124 Corer weight allowed 25-45 cm penetration into the sediment without disturbing the sediment-water interface.

125 Sampling was performed on board the N/O *Côtes de la Manche* anchored at a fixed position. A total of 5

126 sediment cores were simultaneously sampled at each station: 1 core for oxygen profile measurements (n>3), 3

127 cores for porosity, nutrient and metal concentrations in pore waters (n=3), and 1 core for salinity, sulfate and

128 sulfide concentrations in pore waters (n=1). Bottom water samples were taken with a Niskin bottle for oxygen

129 measurement. The transfer of water from the Niskin bottle to the three Winkler bottles was carefully performed

130 avoiding water bubbles. Reagents were immediately added and bottles were closed. Temperature and salinity of

131 overlying waters were recorded immediately after sampling and core were capped and brought back to the main

132 research ship (maximum 1 hour).

133

134 **2.3 Solid-phase analyses**

135 Triplicate sediment cores were immediately sliced at 0.5 cm intervals in the first 2 cm, at 1 cm intervals

136 for 2-4 cm, at 2 cm intervals for 4-12 cm, and at 4 cm intervals for 12-20 cm. An aliquot of the sediment was

137 placed in a vial for porosity measurements. Sediment porosity was determined by drying wet sediment of precise

138 volume at 60°C for 5 days and determining the loss of weight (Berner 1980).

139 The total nitrogen and organic carbon contents were measured in surficial sediments collected in February, May,

140 July and October 2009 for all stations. In February 2009, the 0-0.5 cm depth was measured for all stations, and

141 additionnal the 2-3, 8-10 and 16-20 cm depths were analyzed in intermediate estuaries. As the composition of the

142 upper sediment layer was very homogeneous down to 3 cm, a 50/50 mix of the 0-0.5 and 2-3 cm depth was

143 analyzed for all other cruises. We used an automatic Carlo Erba NA1500 analyser, after removal of the carbonate

144 fraction by dissolution in HCl 1.2N. Organic carbon and total nitrogen concentrations were expressed as the

145 percentage of sediment dry weight (% d.w.). The average standard deviation of each measurement, determined

146 by replicate analyses of the same sample, was ±0.05% d.w. for total nitrogen (TN) and ±0.03% d.w. for organic

147 carbon (OC). Stable isotopic composition of the sedimentary organic carbon ($\delta^{13}C$) was determined with

148 continuous flow FINNIGAN Delta plus XP mass spectrometer, which was directly coupled to the CHN analyser

149 (Gauthier and Hatté 2007). $\delta^{13}C$ values were expressed as the relative difference between isotopic ratios in the

150 sample and in conventional standards (Vienna Pee Dee Belemnite) .

151 $$\delta^{13}C = \left[\frac{(^{13}C/^{12}C)\ sample}{(^{13}C/^{12}C)\ PDB} - 1 \right] \times 1000$$

152 Isotopic results were obtained with uncertainties of $\pm$ 0.2‰ as determined from routine replicate measurements.

153

154 **2.4 Oxygen profiles**

155 On board the ship, sediment cores were immediately placed in a refrigerating loop with a monitoring of

156 temperature and brought back to their initial temperature while bubbled with air. The maximum temperature

157 difference between sampling and ship recovery was < 2°C. The efficiency of the refrigerating loop was increased

158 by the circulation of the overlying water into a cold bath, which brought this water back to the sampling

159 temperature within 1 hour. Oxygen profiles in pore waters were performed on board using Clark type

160 polarographic oxygen microsensors provided with a built-in reference and an internal guard cathode (Revsbech

161 1989). The sensors have an outer tip diameter of 50 µm and were manufactured by Unisense (Århus, DK).

162 The sensors were operated with a motor-driven micromanipulator and the sensor current was measured with a

163 picoamperometer connected to an A-D converter, which transferred the signals to a PC (Revsbech and Jørgensen

164 1986). At each site, a minimum of 3 oxygen profiles was performed in the same core. Linear calibration of

165 microelectrodes was achieved between bottom water oxygenation estimated by Winkler titration (Grasshoff et al.

166 1983) and anoxic (i.e. oxygen-free) sediments. The vertical resolution of measurements was 100-200 µm. The

167 position of the sediment-water interface (SWI) relative to the *in-situ* oxygen profiles was determined using a

168 modified version of the technique of Sweerts and De Beer (1989) which defined the SWI as the first point in the

169 oxygen gradient, after the initial linear oxygen decrease in the diffusive boundary layer, with a slope increase of

170 more than 20%.

171

172 **2.5 Pore water analyses**

173 Sediment aliquots for nutrient, metals and salinity analyses were placed in sealed 50 ml centrifuge tubes

174 containing Vectaspin 20 filters (0.45 µm pore size, Whatman®) according to Andrieux-Loyer et al. (2008). Pore

175 water was extracted by centrifuging at 3075 g for 10 min (2 times) at 4°C and acidified to pH 2 for further

176 nutrient (NO_x^- and NH_4^+) and metal (Fe^{2+}, Mn^{2+}) analyses. NO_x^- and NH_4^+ concentrations were analyzed using

177 segmented flow analysis (SFA; Aminot et al. 2009). Fe^{2+} concentrations were measured with the ferrozine

178 method (Sarradin et al. 2005) and Mn^{2+} concentrations with the leuco-malachite green method (Resing and Mottl

179 1992), both adapted for SFA. The precision of the analysis was 0.5 %.

180 One additional core per site was equipped with Rhizons and polypropylene syringes (Seeberg-Elverfeldt et al.

181 2005), allowing sampling of the pore water at different depth intervals. The Rhizons were placed at 1cm

182 intervals. The pore water collected at the different depths was kept at 4°C until analysis. An aliquot of the sample

183 (200 µl) was distributed in pre-acidified tubes (HCl normapur, 10^{-2} M) for sulfate analysis. $BaCl_2$ plus gelatin

184 reagent was added to precipitate barium sulfate and maintain barite precipitate in suspension. Turbidity was

185 recorded at 470 nm (Tabatabai 1974). A sample fraction for ΣH_2S analysis (200 µl) was immediately transferred

186 to a tube containing 3 ml of a trap solution consisting of zinc chloride (1.5×10^{-2} M) and gelatin (3g l^{-1}) to

187 precipitate ZnS (preventing sulfide oxidation and gas loss). When necessary, samples were diluted with NaCl

188 stock solution whose composition matched surface seawater salinity. Total hydrogen sulfide concentrations were

189 measured by the methylene blue method (Merck Spectroquant® 14779; λ=660 nm). Standards were prepared

190 with a daily made Na_2S stock solution (~10 mM). Salinity was measured by conductivity against a S=35 OSIL

191 standard.

192

193 **2.6 Diffusive oxygen flux calculations**

194 Diffusive oxygen uptake (DOU) was calculated from O_2 concentration gradients at the sediment–water

195 interface by using the 1-D Fick's first law of diffusion: $DOU = \varphi\, D_s \left[\dfrac{dO_2}{dx} \right]_{x=0}$ where φ is the porosity, D_s is

196 the O_2 diffusion coefficient within the sediment and $\left[\dfrac{dO_2}{dx} \right]_{x=0}$ is the oxygen gradient just below the sediment–

197 water interface (estimated from the profiles). D_s was estimated as $D_s = \dfrac{D_{0_{O_2}}}{\varphi^2}$. $D_{0_{O_2}}$ is the molecular diffusion

198 coefficient of O_2 (cm² s^{-1}) at *in situ* temperature, salinity and hydrostatic pressure and was evaluated using tables

199 from Broecker and Peng (1974). The oxygen gradient was estimated over 400 to 600 microns depending on the

200 resolution of the profiles.

201 In order to establish a seasonal comparison of fluxes without temperature effect, O_2 fluxes obtained previously at

202 *in situ* temperature were all recalculated for a standard temperature of 10°C. A temperature coefficient Q_{10} was

203 applied to the O_2 fluxes. The Q_{10} represents the factor by which the bacterial activity increases for a rise of 10°C

204 by the temperature (Thamdrup et al. 1998). This rate corresponds to the diffusive demand of oxygen related to

205   the bacterial mineralization activity and a value of Q_{10} of 2.5 was assumed. The diffusive demand of oxygen at a

206   given temperature T (DOU_T) was obtained using:

207    $$DOU_T = \frac{DOU_{Ti}}{2.5^{\left(\frac{T+10}{10}\right)\left(\frac{Ti-T}{Ti}\right)}}$$ eq.1

208   Where $Q_{10} = 2.5$, DOU_{Ti} is the diffusive demand of oxygen at initial temperature Ti, Ti the initial temperature

209   and T the final temperature.

210

211   **2.7 Statistical analyses**

212   Non-parametric Mann Whitney tests were used to compare oxygen penetration depths (OPD) and fluxes

213   at different stations in each estuary and the potential seasonal differences of OPD and fluxes for a given station.

214   We used the non-parametric Kruskal Wallis test to check the differences between stations in each estuary or

215   between seasons for a given station. The Mann Whitney test was used to define which station (or season) was

216   different from the other. For all tests, statistical differences were significant for $p < 0.05$. The station E1 in

217   February was not included in the statistics because only one profile was measured.

218

219   **3   Results**

220   **3.1 River parameters**

221   Wind speed amplitude, frequency, precipitations and river discharges were higher during winter and fall

222   than in spring and summer (Raimonet 2011). For each estuary and at each season, sampling was undertaken at

223   three different stations along the salinity gradient. Environmental parameters for each station and season are

224   given in Table 1 and are described below. The high winter Elorn and Aulne river discharges increased up to 30

225   and 130 m^3 s^{-1}, respectively, at the beginning of sampling in February, and decreased by a factor > 2 at the end of

226   the sampling period. The Aulne River discharge was higher than the Elorn River discharge by a factor of ~ 3

227   during winter but similar or occasionally lower during summer.

228   In each estuary, the inner station was generally characterized by freshwater (salinity=0; Table 1) and brackish

229   waters in October. The mid station was located in the mixing zone between fresh riverine water and salt water

230   with a salinity ranging from 13-17 in February to 30 in October. The outer station was located near the mouth of

231   each estuary and presented an average salinity higher than 20 and 30 in the Elorn and Aulne estuaries,

232   respectively. The salinity at the outer station was always higher in the Elorn than the Aulne Estuary. As these

estuaries are shallow, samplings in subtidal shores were carried out between 1 and 8 m depth. The bottom water temperatures followed a seasonal pattern and varied between a minimum of 7.4°C in February and a maximum of 19.7°C in July. The water temperatures were similar in the Elorn and Aulne estuaries during the different seasons. We observed a decrease in bottom water O_2 concentrations from February to October for both estuaries. The water O_2 concentrations were higher in the Aulne than Elorn Estuary, except in May.

3.2 Variability at small spatial scales

Spatial variations were studied at various small scales in May 2009 in the mid Elorn Estuary (station E2), at the centimeter scale (intra-core O_2 profiles and fluxes), at the meter scale (triplicate cores #1, #2 and #3) and along the cross-river section (stations E2, b, c, d and e). Fig.2 shows vertical profiles of O_2, NO_x^-, NH_4^+, Fe^{2+} and Mn^{2+} concentrations and diffusive O_2 uptakes (DOU) calculated at the centimeter and meter scales (left panels) and along the cross-section (right panels). Similar variability of O_2, nutrient and metal profiles were observed at the centimeter and meter scales and along the cross-section. Oxygen penetration depth (OPD) and DOU observed in a core sampled at station E2 (OPD: 1.7-2.5 mm; DOU: 23 ± 1 mmol m^{-2} day^{-1}; Fig.2a) were similar to the values measured along the transversal estuarine section (OPD: 1.7-2.1 mm; DOU: 20-22 mmol m^{-2} day^{-1}). The penetration depth of NO_x^- was always 1.5-2.5 cm depth (Fig.2c). The same trends were observed for the vertical profiles of NH_4^+, PO_4^{3-} and $Si(OH)_4$ concentrations (the two latter are not shown; see Raimonet et al. in review) regardless of the small spatial scale. Pore water NH_4^+ concentrations increased with depth with a lower concentration gradient generally observed between 6 and 12 cm depth. Pore water NH_4^+ concentrations were in the range of 20-250 µM except at deeper depth where concentrations reached up to 1000 µM at 18 cm at station E2. The lowest NH_4^+ concentrations were measured in and around the channel (at stations b, c, d), whereas the highest concentrations were measured in subtidal shores (at 0-8 cm depth at station e, and below 8 cm at station E2). Maximal Mn^{2+} concentrations were always observed between 0 and 2 cm depth. Low variations in the vertical Mn^{2+} profiles were observed at all stations, except higher Mn^{2+} concentrations in the first 1.5 cm depth in the channel (note that there is no data between 1.5 and 6 cm). The vertical Fe^{2+} concentration profiles were more variable than other elements at the centimeter and meter scale and along the transversal section. The shape of the vertical Fe^{2+} concentration profiles was however similar with concentration peaks observed down to the maximal Mn^{2+} concentrations. As for NH_4^+ concentrations, the lowest Mn^{2+} concentrations were observed close to the channel.

263 **3.3 Intra- and inter-estuary spatial variability**

264   **3.3.1 Porosity and salinity**

265   Porosity generally decreased with depth at all stations in February and May, ranging between 0.67-0.95

266 regardless of stations and seasons (Fig.3). Several vertical discontinuities were observed however in the inner

267 and mid Elorn Estuary in February and in the mid and outer Aulne Estuary in May. Salinity slightly increased

268 with depth at all stations in February and in the inner Elorn Estuary (E1) in May. Except for station E1, salinity

269 was constant over depth at all stations in May (Fig.4). In both estuaries, salinity increased from the inner to the

270 outer estuaries.

271

272   **3.3.2   Organic carbon and isotopic composition in surface sediments**

273   Both estuaries had similar organic carbon contents in February and showed large variations along the

274 salinity gradient during the other seasons (Fig.5a and b). Low organic carbon contents were observed in outer

275 estuaries (stations E3 and A3). Most organic carbon contents ranged between 1.5 and 6.0% d.w. in both

276 estuaries, with higher values (~7.0% d.w.) at E1 in July and at A2 in October. Organic carbon contents generally

277 decreased downstream, except in October in both estuaries and in July in the Elorn Estuary where the mid

278 brackish station showed a larger organic carbon content than the upper freshwater station. Organic carbon

279 contents were always lower at the outer than upper stations.

280 The Fig.5c and d show the carbon to nitrogen molar ratios (C/N) in surficial sediments for the different seasons.

281 Inner and mid estuaries (stations 1 and 2) displayed similar C/N ratios $\geq$ 10, except in the Elorn Estuary in

282 October. Outer estuaries (station 3) always showed values $\leq$9 in the Elorn Estuary and between 9 and 11 in the

283 Aulne Estuary.

284 $\delta^{13}C$ values were generally higher in the Elorn than the Aulne Estuary (Fig.5e and f). $\delta^{13}C$ values were

285 similar in all seasons in the inner and mid Elorn and Aulne estuaries, except in October in the Aulne Estuary.

286 The outer estuary (station 3) showed higher values than inner and mid stations for both estuaries, this difference

287 being larger in the Elorn than the Aulne Estuary. $\delta^{13}C$ values were seasonally stable in the Elorn Estuary,

288 whereas they showed a 0.6-0.7‰ decrease from February to October in the Aulne Estuary.

289

290   **3.3.3   Oxygen profiles**

291   The O_2 bottom water concentrations (O_{2bw}) decreased by about 20 % along the salinity gradient in each

292 estuary in February (Fig.6a and b). At other seasons, except in July in the Aulne Estuary, there was a decrease

293 from inner to mid estuaries but low variations in the outer estuaries (Fig.6c and h). The decrease in O_{2bw}

294 concentrations slightly coincided with a decrease in the thickness of the oxic zone.

295 The O_2 penetration depth was low and varied from 1.15 ± 0.10 mm at E2 in February to 5.10 ± 0.42 mm at A3 in

296 February. Overall, the O_2 penetration depths were larger in the Aulne than the Elorn Estuary (Fig.6i and j).

297 Penetration depths of O_2 were generally lower at mid stations (A2 and E2) than outer stations (A3 and E3).

298 There was a difference between the inner estuary stations of the Aulne and Elorn estuaries. In the inner estuaries,

299 the penetration depth of O_2 was larger in the Aulne (A1) than Elorn sediments (E1). Penetration depths of O_2

300 were only slightly higher at the inner station E1 than at the mid station E2. There was no seasonal trend for O_2

301 penetration depth in sediments of these two estuaries.

302

3.3.4 Nutrient and metal profiles

304 Inorganic oxidized nitrogen (NO_x^-) concentrations in the overlying water (Fig.7a and b, 8a and b) were

305 the highest in the inner and mid Elorn stations, varying between 500-520 µM (E1) and 150-498 µM (E2). Lower

306 concentrations, between 7 and 63 µM, were measured in the outer estuary (E3). In addition to this difference

307 along the estuary, NO_x^- concentrations decreased between February and May for the inner and intermediate

308 stations E2 and E3. In the Aulne Estuary, pore water NO_x^- concentrations decreased from inner estuary (A1: 145-

309 250 µM) to outer or mid estuary (around 30-100 µM) and from February to May at A1 and A3. An increase from

310 February to May was observed at A2 (from 13 to 65 µM).

311 Pore water NO_x^- profiles exhibited similar patterns in the Elorn and Aulne estuaries (Figs.7c and d, 8c and d). All

312 pore water NO_x^- profiles showed a strong decrease in concentrations with depth. At all stations, NO_x^-

313 concentrations were below the detection limit at a depth of 1-4 cm in February and below 1-2 cm depth in May.

314 The lowest NO_x^- penetration depths occurred in the mid and outer Elorn Estuary (E2 and E3). Little seasonal

315 variation regarding the NO_x^- pore water profiles was observed at stations E2 and E3. In the Aulne Estuary,

316 elevated NO_x^- concentrations were determined in the bottom water and top 1 cm of sediment, whereas below the

317 detection limit at depth (below 2-4 cm). The lowest penetration depths of NO_x^- were observed in May.

318 For all sites in the Elorn and Aulne estuaries, the concentration of Fe^{2+} in the overlying water was lower than 3

319 µM (Figs.7e and f, 8e and f). The pore water profiles of Fe^{2+} were characterized by an increase at depth

320 coinciding with the depth at which NO_x^- disappeared. Below this depth, in the Elorn Estuary, Fe^{2+} concentrations

321 up to 200 µM (E2, E3) and 50 µM (E1) were detected. At deeper depth, Fe^{2+} concentrations decreased and were

322 absent below 5 cm depth. Furthermore, little seasonal variation was observed regarding the pore water Fe^{2+}

323 profiles. Pore water Mn^{2+} were very similar to the Fe^{2+} depth profiles, with 20 fold lower concentrations. The

324 Fe^{2+} pore water profiles showed a larger variability in the Aulne compared to the Elorn Estuary. A typical

325 subsurface peak, as in the Elorn Estuary, was observed in the outer station (A3, 200 µM). A similar depth profile

326 was also present at the intermediate station (A2), however the Fe^{2+} concentrations reached values up to 1500 µM

327 (February) and 2000 µM (May). No typical subsurface peak in Fe^{2+} was observed in the inner estuary (A1); pore

328 water Fe^{2+} concentrations gradually increased up to 14 cm depth at A1 (700 µM). Profiles of pore water

329 Mn^{2+} concentrations displayed similar patterns, with a subsurface peak, as Fe^{2+}, at 50 fold lower concentrations.

330 In contrast to the Fe^{2+} concentrations, Mn^{2+} was still present at deeper depth.

331 Overall NH_4^+ concentrations were low in the overlying water at the different locations in the Elorn Estuary as

332 well as throughout the different seasons (<10 µM; Figs.7g and h, 8g and h). The pore water profiles of NH_4^+

333 concentrations gradually increased from 10-20 µM in the surficial sediment up to 1200 µM in the deeper layers.

334 In February, NH_4^+ profiles displayed a greater spatial variability; the mid station (E2) showed a particular pattern

335 with concentrations about 2 to 6 times higher than at E1 and E3 and about 2 times higher in February than in

336 May (up to 2400 µM). In the inner estuary (E1), NH_4^+ concentrations, at deeper depth, increased from 400 µM in

337 February to 900 µM in May. In the outer estuary (E3), concentrations were similar in February and May. Similar

338 to the Elorn Estuary, NH_4^+ profiles (February) showed concentrations in the inner estuary (A1) up to 2.5 times

339 higher than in the mid and outer estuary (A2 and A3) and higher than in May. In May, NH_4^+ profiles showed

340 similar patterns than in the Elorn Estuary, with little spatial variability and concentrations increasing with depth

341 up to 1200 µM in the outer estuary (A3).

342 SO_4^{2-} concentrations in the overlying water were low in the inner Elorn and Aulne estuaries (~5 mM; Fig.7i and

343 j) and high in the mid (10-18 mM) and outer estuary (18-31 mM). Similar trends were observed in May (Fig.8i

344 and j). Little variation in these concentrations was observed with depth in the inner and mid Elorn Estuary,

345 whereas a decrease at deeper depth was observed at the outer station (E3). High and comparable SO_4^{2-}

346 concentration profiles were measured at the mid and outer Aulne estuary, decreasing from 20 mM at the

347 sediment-water interface to 14 mM at 12 cm depth (Figs.7j and 8j).

348 No H_2S was detectable in the Elorn and Aulne sediments in February (Fig.7k and l). In May, H_2S concentrations

349 were below the detection limit in the top layers of the sediment and at the intermediate station (E2; Fig.8k).

350 Concentrations of H_2S up to 40 µM were detected at a depth below 5 cm at the inner station (E1). At the outer

351 station (E3), concentrations increased with depth below 16 cm and reached up to 100 µM at 20 cm. H_2S

352 concentrations in the Aulne estuary were low in May, with only traces measured at the mid station (A2; Fig.8l).

3.4 Seasonal variability of diffusive O$_2$ fluxes

354   The mean diffusive O$_2$ fluxes calculated at the three stations in the Elorn and Aulne estuaries and at each

355   season are shown in Fig.9a and b. In both estuaries except mid stations, diffusive O$_2$ fluxes were higher in May

356   and July than in February and, in a smaller extent, in October. At mid stations (E2 and A2), diffusive O$_2$ fluxes

357   were similar over the year, with a small drop in October.

358   The diffusive O$_2$ fluxes recalculated for a temperature of 10°C using the temperature Q$_{10}$ relationship (Thamdrup

359   et al. 1998) for each station and season are presented in Fig.9c and d. In the Elorn and Aulne estuaries, we

360   observed higher T-corrected (Fig.9c and d) than not corrected (Fig.9a and b) diffusive O$_2$ fluxes in February but

361   lower T-corrected diffusive O$_2$ fluxes in May, July and October. Once normalized to a fixed temperature, the

362   seasonal variation with larger values in spring and summer was smoothed out at station E1, E3 and A3. Some

363   inverse decreasing trend from February-May to July-October appeared at stations E2, A1, A2.

364

365   **4   Discussion**

366   **4.1 Benthic heterogeneity at station and cross-estuary scales**

367   The similarity of the vertical profiles of O$_2$, nutrient and metal concentrations at the station scale (within

368   meters of the exact location) and cross-section scale highlights the relative homogeneity of benthic properties in

369   the mid estuary. This low heterogeneity at the station scale allows temporal variability to be studied. The

370   variability of pore water profiles of NH$_4^+$, Fe^{2+} and Mn^{2+} at the cross-section and station scales is much lower

371   than the variability observed between estuaries and along salinity gradients. The low cross-section variability

372   observed in this study suggests thus that biogeochemical heterogeneity might be low in estuaries characterized

373   by a small channel width, contrary to higher variations observed in larger systems (e.g. Hammond et al. 1985;

374   Grenz et al. 2000), or by measurements of net benthic fluxes that integrate all benthic processes (Hammond et al.

375   1985; Thouzeau et al. 2007).

376   Although O$_2$ variability is low in the whole cross-section, nutrient and metal concentrations are slightly lower in

377   the channel compared the subtidal shores, suggesting slight differences in benthic biogeochemical processes.

378   Channel sediments might have been characterized by lower organic matter inputs and benthic macrofauna

379   activity (as already suggested by benthic fluxes measurements in San Francisco Bay; Hammond et al. 1985),

380   which could have led to slower diagenetic processes in the channel. It is worth noting that opposite trends can be

381   observed in larger and more productive areas where benthic remineralization is higher in the channel compared

382   to the shoal (Grenz et al. 2000).

383   The relatively low variability of benthic pore water properties is however in contrast with general high benthic

384   heterogeneity due to processes that occur in surficial sediments in coastal ecosystems, e.g., heterogeneous

385   distribution of benthic macrofauna and/or primary producers, sediment porosity variability, microtopography,

386   local deposition of labile organic matter, micro-scale turbulence, and resuspension–deposition events (Huettel et

387   al. 2003; Rabouille et al. 2003, Glud 2008; Mügler et al. 2012). The heterogeneity is sometimes high enough to

388   prevent the study of seasonal variations (Bay of Biscay; Mouret et al. 2009). The results of our study show that

389   benthic heterogeneity in inner estuarine sections characterized by a small channel area is low. The low variability

390   of triplicate profiles and fluxes of O_2 and the sampling at the same station on the left subtidal shore allows

391   studying seasonal variations of diffusive O_2 fluxes in the two estuaries.

392

393   **4.2 Seasonal variations at the estuary scale**

394   Increases in salinity from winter to spring have to be considered with respect to hydrologic records. For

395   instance, the average daily discharge in the Aulne River ranged between 100 and 200 $m^3 s^{-1}$ in January-February

396   2009 but only 20 $m^3 s^{-1}$ in April-May. In the Elorn River, average daily discharge dropped from 12-30 $m^3 s^{-1}$ to 5

397    $m^3 s^{-1}$.

398   If pore water salinity is a good tracer of overlying water salinity and thus of seasonal hydrological conditions,

399   pore water chemical composition would respond at least partially to seasonal changes. Especially, the rate of

400   sulfate reduction most likely increases in May, not only due to temperature changes, but also due to higher

401   sulfate resupply still observable in the mid Elorn Estuary in May. Higher sulfate reduction rates in sediment or

402   lower sulfide control by FeS precipitation lead to higher H_2S concentration in pore waters in May, especially in

403   the Elorn Estuary. However, for electron acceptors ubiquitously present in fresh or marine waters (O_2, NO_3^-,

404   MnO_2, FeOOH), diffusive and advective supplies (in zones of coarser sediments) related to salinity changes will

405   have little effect on early diagenetic processes related to those chemical species. This statement may provide an

406   explanation for the lack of significant seasonal variation regarding ammonium profiles. Consequently, variability

407   of early diagenesis processes in and between those two estuaries is expected to be controlled by organic matter

408   deposition and seasonal changes in temperature rather than salinity changes.

409   The role of the benthic fauna on oxygen profiles and diffusive fluxes might have been limited in this study, even

410   if benthic fauna was present in these estuaries (except at stations A1 and A2; Michaud pers. comm.; Raimonet

411   2011). The presence of benthic fauna has already been shown to increase total benthic oxygen fluxes depending

412   on the bioturbation strategy and feeding activity which vary among species (Michaud et al. 2005). Here, we

413 report diffusive oxygen uptake, i.e. when measurements of oxygen profiles were performed in sediments out of

414 animal burrows in order to avoid the interference with benthic fauna. The similarity between replicate oxygen

415 profiles and the absence of vertical discontinuities in oxygen profiles confirms the homogeneity of the sediments

416 with regards to the diffusive uptake of oxygen.

417 Overall, sediment oxygen demands are larger in the Elorn compared to the Aulne estuarine sediments. The

418 seasonal trend is well marked with an increase during spring and summer (May and July) for all stations, except

419 in the mid Elorn Estuary. Sediment oxygen demand is lower during winter and fall (February and October). This

420 seasonal variation gives rise to a bell-curve pattern for the temporal evolution at each station (Fig.9). This pattern

421 is largely related to the seasonal evolution of temperature typically observed in mid-latitude regions (Dedieu et

422 al. 2007). In this temperate and oceanic system, temperature in the bottom estuarine water increases by 10°C

423 between <8°C in winter and 18°C in summer (Table 1). Temperature increases diffusion coefficients as well as

424 aerobic microbial activity resulting in higher oxygen fluxes.

425 The lower seasonal variations of oxygen fluxes at intermediate salinities (E2 or A2) suggest that other factors,

426 such as organic carbon loading and dissolved oxygen concentrations, might vary at the seasonal scale and

427 decrease the range of seasonal variations in the benthic oxygen demand. Oxygen fluxes were thus normalized to

428 a common temperature of 10°C in order to limit the temperature effect and estimate the influence of other

429 parameters. T-corrected diffusive oxygen fluxes show a different seasonal variation than diffusive oxygen fluxes

430 calculated at *in situ* temperature (Fig.9c and d). They indicate a relatively stable trend for stations E1, E3 or A3,

431 whereas a clear and progressive seasonal decrease from February to October is observed for mid stations E2 and

432 A2 and, to a lesser extent, at the upper station A1. The change in oxygen concentration in the bottom water,

433 largely due to seasonal changes in temperature and salinity, partly explains this decrease with time. It is known

434 that oxygen concentration in bottom waters influences oxygen fluxes as they mechanically decrease the gradient

435 for a given microbial consumption in the sediment (Hall et al. 1989; Rabouille and Gaillard 1994; Cai et al.

436 1995). Yet, this dependence is small if the oxygen concentration in the bottom water remains above 75 µM (Cai

437 et al. 1995). In the two mid estuaries where the decrease in oxygen flux is the most pronounced, oxygen

438 concentrations and diffusive T-corrected oxygen fluxes are closely linked (r^2 = 0.95). However, the observed

439 sensitivity of the T-corrected diffusive oxygen flux to the oxygen concentration change during the year is very

440 high as T-corrected diffusive oxygen fluxes are divided by 3 or more for a reduction of oxygen by only 100-150

441 µM (30-40% of the initial value). This large decrease of O_2 fluxes points towards other processes correlated to

442 the seasonal decrease in oxygen concentration, such as changes in organic matter input or its reactivity.

443   Contrasted temporal variations of T-corrected diffusive oxygen fluxes in the Elorn and Aulne estuaries suggest

444   differences in the factors controlling the seasonal variations of benthic diffusive oxygen flux. In the Elorn

445   Estuary, T-corrected diffusive oxygen fluxes decrease from upstream to downstream at most seasons except in

446   February where a peak at intermediate salinity (E2) occur. At station E2, a large temporal variability of T-

447   corrected fluxes along the year is observed as fluxes vary from 10 to 25 mmol m^{-2} day^{-1}. The situation is

448   different in the Aulne Estuary where T-corrected sediment oxygen fluxes are rather constant from the inner to

449   outer estuary with lower seasonal variability at each station. Both the large seasonal variations of benthic

450   diffusive oxygen flux and its spatial pattern along the estuaries suggest that a large input of labile organic matter

451   occurring during the winter might be slowly mineralized during the year at the mid estuary as it has already been

452   shown in different estuarine, coastal and marine environments (Gehlen et al. 1997; Cathalot et al. 2010, Cathalot

453   et al. 2012). This phenomenon more pronounced in Elorn that in Aulne Estuary, might be correlated with the

454   oxygen reduction in bottom water, and would provide the spatial pattern observed in Fig.10. In addition, if this

455   effect is lower in the Aulne Estuary, then lower oxygen fluxes are expected as currently observed. Clearly, a

456   modelling approach is needed to disentangle the various forcing on organic matter mineralization which is the

457   driving force of oxygen fluxes in these sediments.

458

459   **4.3 Organic matter flux and quality**

460   In temperate estuaries and deltas, the origin of organic matter and its potential reactivity is complex and

461   is linked to different types of organic matter: terrestrial, riverine, marine and urban waste (Cifuentes et al. 1988;

462   Barth et al. 1998; Hellings et al. 1999; Lansard et al. 2009; Xiao and Liu 2010; Pastor et al. 2011b). In estuarine

463   environments, the composition of organic matter in the upper sediment layer that is mineralized responds

464   seasonally to the changes in the composition of suspended particles.

465   In the Aulne and Elorn estuaries, a seasonally reproducible pattern of organic carbon content, C/N ratio and $\delta^{13}C$

466   is found along the estuary (Fig.5). Organic carbon content and C/N ratio are high in upper sediments (4-6% d.w.

467   and 11-15, respectively) and decrease downstream to values around 2% d.w. and C/N≤10. The amplitude of this

468   seaward decrease varies with the season. It is less pronounced in winter and increases in spring, summer and fall.

469   The decrease of organic carbon content and C/N ratio suggests that the carbon transported by the rivers into the

470   estuaries is diluted, mineralized and mixed with marine organic carbon characterized by lower C/N, typically

471   around 7-8 for fresh phytoplankton (Tesi et al. 2007; Lansard et al. 2009). The carbon isotopic composition also

472   shows a stable pattern throughout the seasons and in the two estuaries. The $\delta^{13}C$ of organic carbon increases

473   seaward from similar values in the inner parts of the two estuaries to significantly higher $\delta^{13}C$ in outer estuaries.

474   The simultaneous increase of $\delta^{13}C$ and decrease of C/N confirm the seaward increase in marine organic material.

475   A plot of N/C against $\delta^{13}C$ shows a clear mixing trend between two end-members: (1) plant debris and soil

476   organic matter with lower N/C and $\delta^{13}C$, and (2) marine phytoplankton with larger N/C and $\delta^{13}C$ (Fig.11). A

477   difference in the absolute values of $\delta^{13}C$ and N/C however appears between the two estuaries, the organic matter

478   showing always lower $\delta^{13}C$ and N/C values in the Aulne than the Elorn Estuary. This could be biased by the fact

479   that the outer Elorn station (E3) showed consistently larger salinities than the outer Aulne station (A3),

480   indicating a higher contribution of marine organic matter. However, the addition of a station further downstream

481   of the Aulne Estuary (A4, Fig.11) at salinity similar to the outer Elorn station, still showed lower values than the

482   outer Elorn station (N/C $\approx$ 0.12 and $\delta^{13}C \approx$ -24.5‰). The difference in the organic carbon signature in surface

483   sediments between the two estuaries points thus rather towards a different origin of organic matter. Plants and

484   soils are very similar in the two drainage basins that are geographically, climatically and geologically close. A

485   difference between both drainage basins exists however in the human activities and the river morphology and

486   hydrology (Fraisse et al., submitted). The Elorn River drains a mixed countryside and small cities watershed

487   (220 inhabitants km^{-2}) with intensive pig and caw farming and important river channelling. The Aulne watershed

488   is characterized by agricultural activities and numerous dams and river locks. Therefore, the Elorn River has

489   little production of riverine plankton because of the short residence time of the water although nutrient

490   concentrations are high and receives sewage/farm organic matter inputs. The Aulne Estuary shows larger values

491   of chlorophyll *a* in its upper reaches and in the estuary itself (Fraisse et al., submitted), and may carry a larger

492   proportion of river phytoplankton into the estuary.

493   The isotopic and elemental signature of sewage organic matter are close to the mix of terrestrial plants and soils

494   (Ruiz-Fernández et al. 2002; Xiao and Liu 2010), as sewage inputs show $\delta^{13}C$ of -25‰ and C/N of 12 (N/C =

495   0.08). These values are typically observed in the Elorn Estuary (Fig.5), which highlight the possible load of

496   sewage and the similar contents of terrestrial and marine matter. In order to explain lower $\delta^{13}C$ in the Aulne

497   Estuary, it is noteworthy that phytoplankton is dependent on the $\delta^{13}C$ of dissolved inorganic carbon (DIC) in the

498   river in which they grow. As Brittany rivers contain low DIC due to the granitic nature of watershed, $\delta^{13}C$ of

499   DIC may be largely influenced by remineralization in the river and may produce negative values, thus lowering

500   the $\delta^{13}C$ of riverine phytoplankton as shown in the Delaware estuary (Cifuentes et al. 1988). The differential

501   input of sewage (-25‰) in the Elorn estuary and phytoplankton (maybe as low as -28‰) in the Aulne estuary

502   may explain the lower $\delta^{13}C$ values in the organic carbon of the Aulne Estuary versus the Elorn Estuary.

4.4 Organic matter mineralization in estuaries

Overall, the release of NH_4^+ during the organic matter degradation is reflected by an increase in concentration with depth (e.g Berg et al. 2003; Canavan et al. 2006). Comparable NH_4^+ pore water profiles, with a few exceptions, regardless stations and seasons suggest similar organic matter mineralization rates per station during the different seasons for both estuaries. Higher NH_4^+ concentrations observed in February at stations E2 and A1 indicate higher anaerobic mineralisation rates at these two stations, which is also highlighted by the formation of authigenic phosphorus in the upper Aulne Estuary (Raimonet et al. in review).

The pore water profiles and associated diffusive fluxes of O_2 indicate slightly higher aerobic organic matter degradation in the Elorn compared to the Aulne Estuary, which highlight more reactive organic matter in the top layers in the Elorn Estuary. The high NO_3^- concentrations in the overlying water, larger than oxygen concentration in these NO_3^--rich estuarine waters, especially in the inner estuaries, most likely contribute largely to organic matter degradation in the oxic to suboxic top layer (e.g. Berg et al. 1998). The contribution of NO_3^- reduction to organic matter mineralisation is less important in the outer estuary, due to lower concentrations in the overlying water.

In the deeper anoxic layers, below the oxygen and nitrate penetration depths, iron and manganese oxides and sulphate play a role in the further degradation of the organic matter. The low concentrations of reduced Fe^{2+} and Mn^{2+} at depth in the Elorn Estuary compared to the Aulne Estuary indicate a limited contribution of metal oxides in the organic matter mineralisation. Higher pore water concentration of iron and manganese are observed in the Aulne Estuary (especially at the intermediate station), resulting in a higher contribution of Fe and Mn oxides to anoxic mineralisation of organic matter. High SO_4^{2-} concentrations in the overlying water and a decrease in the pore waters in the mid and outer sediments of the Aulne Estuary for example suggest a role of SO_4^{2-} reduction in the mineralisation of the organic matter. This is confirmed by the slight decrease in SO_4^{2-} concentrations (with a few exceptions) and the production of H_2S (E1, E3 May) at deeper depth. The production of H_2S during SO_4^{2-} reduction and the absence of this compound at deeper depths can be explained by the precipitation of HS^- with Fe^{2+}.

In order to establish quantitative estimations of the different processes contributing to the degradation of organic matter a modelling approach is needed.

5 Conclusion

In this paper, we determined the spatio-temporal distribution of benthic oxygen, pore water nutrients and metals along the salinity gradients during four seasons. The variability of pore water profiles of NH_4^+, Fe^{2+} and Mn^{2+} at the cross-section and station scales is much lower than the variability observed between estuaries and along salinity gradients. The low cross-section variability observed in this study suggests thus that biogeochemical heterogeneity might be low in estuaries characterized by a small channel width. Overall, sediment oxygen demands are larger in the Elorn compared to the Aulne estuarine sediments. Suboxic and anoxic organic matter mineralization is variable over the seasons and indicates large nitrate consumption, large anoxic mineralization as exemplified by pore water NH_4^+ gradients in both estuaries and sulphate reduction in the Elorn Estuary. The role of metal oxides in early diagenesis seems to be limited but interactions with other compounds such as sulphide may limit their concentration. Organic carbon and nitrogen analyses indicate that the origin of carbon is different in the two watersheds with lighter $\delta^{13}C$ of carbon in the Elorn watershed linked to urban sewage or farm inputs. The lability of these inputs could lead to larger mineralization in upstream stations of this estuary compared to the Aulne Estuary. A modelling approach is needed to quantify the relative strength of the different early mineralization pathways and understand the forcing on organic matter mineralization in these contrasted estuaries.

References

Aminot A, Kerouel R, Coverly SC (2009) Nutrients in seawater using segmented flow analysis, CRC Press, Boca Raton, pp 143–178

Andrieux-Loyer F, Philippon X, Bally G, K´erouel R, Youenou A, Le Grand J (2008) Phosphorus dynamics and bioavailability in sediments of the Penz´e Estuary (NW France): in relation to annual p-fluxes and occurrences of Alexandrium minutum. Biogeochemistry 88(3):213–231

Barth JAC, Veizer J, Mayer B (1998) Origin of particulate organic carbon in the upper St. Lawrence: isotopic constraints. Earth Planet Sci Let 162: 111-121

Berg P, Risgaard-Petersen N, Rysgaard S (1998) Interpretation of measured concentration profiles in sediment pore water. Limnol Oceanogr 43: 1500–1510

567 Berg P, Rysgaard S, Thamdrup B (2003) Dynamic modeling of early diagenesis and nutrient cycling. A case
568 study in an Arctic marine sediment. American Journal of Science 303: 905-955
569
570 Berner RA (1980) Early diagenesis: A Theoretical Approach. Princeton University Press, 241 pp
571
572 Bopp RF, Simpson HJ, Olsen CR, Trier RM, Kostyc N (1982) Chlorinated hydrocarbons and radionuclides
573 chronologies in sediments of the Hudson river and estuary, New York. Environ. Sci. Technol. 16: 666-676
574
575 Broecker WS, PENG TH (1974) Gas exchange rates between air and sea. Lamont-Doherty Geological: 21-35
576
577 Burgin AJ, Hamilton SK (2007). Have we overemphasized the role of denitrification in aquatic ecosystems? A
578 review of nitrate removal pathways. Front. Ecol. Environ. 5(2): 89–96
579
580 Cai WJ, Reimers CE (1995) Benthic oxygen flux, bottom water oxygen concentration and core top organic
581 carbon content in the deep northeast Pacific ocean. Deep-Sea Res. 42: 1681-1699
582
583 Canavan RW, Slomp CP, Jourabchi P, Van Cappellen P, Laverman AM, Van den Berg GA (2006) Organic
584 matter mineralization in sediment of a coastal freshwater lake and response to salinization. Geochimica Et
585 Cosmochimica Acta 70: 2836-2855
586
587 Canfield DE, Jorgensen BB, Fossing H, Glud R, Gundersen J,Ramsing NB, Thamdrup B, Hansen JW, Nielsen
588 LP, Hall POJ (1993) Pathways of organic carbon oxidation in three continental margin sediments. Marine
589 Geology 113(1-2): 27-40
590 Cathalot C, Rabouille C, Pastor L, Deflandre B, Viollier E, Buscail R, Grémare A, Treignier C, Pruski A (2010)
591 Temporal variability of carbonrecycling in coastalsedimentsinfluenced by rivers: assessing the impact of flood
592 inputs in the Rhône River prodelta. Biogeosciences 7: 1187-1205
593
594 Cathalot C, Lansard B, Hall Per OJ, Tengberg A, Almroth-Rosell E, Apler A, Calder L, Bell E, Rabouille C
595 (2012) Loch Impacted by Fish Farming: A Combination of In Situ Techniques. Aquat. Geochem.
596 doi:10.1007/s10498-012-9181-4
597
598 Cifuentes LA, Sharp JH, Fogel ML (1988) Stable carbon and nitrogen isotope biogeochemistry in the Delaware
599 estuary. Limnol. Oceanogr. 33: 1102-1115
600 Cloern JE (1996) Phytoplankton bloom dynamics in coastal ecosystems: A review with some general lessons
601 from sustained investigation of San Francisco Bay, California, Rev. Geophys. 34: 127-168,
602 doi:110.1029/1096RG00986
603

604   Cloern JE, Jassby AD (2012) Drivers of change in estuarine-coastal ecosystems: Discoveries from four decades
605   of study in San Francisco Bay. Rev. Geophys. 50, RG4001, doi:4010.1029/2012RG000397

606

607   Deflandre B., Mucci A, Gagné JP, Guignard C, Sundby B (2002) Early diagenetic processes in coastal marine
608   sediments disturbed by a catastrophic sedimentation event. Geochim Cosmochim Acta 66 : 2547-2558

609

610   Del Amo Y (1996) Dynamique des structure des communautés phytoplanctoniques en écosystèmes côtiers
611   perturbé ; cinétique del'incorporation du silicium par les diatomées. Thèse de Doctorat, Université de Bretagne
612   Occidentale, Brest

613

614   Fraisse S., M. Bormans,Y. Lagadeuc (submitted) Phytoplankton community in rivers: a morphofunctional traits
615   approach submitted Aquatic Ecology

616

617   Gauthier C, Hatté C (2007) Suitability and reliability of isotopic biogeochemistry studies in paleoclimatology:
618   focus on protocols. In Geophysical Research Abstracts EGU 2007 02912

619   Gehlen M., Rabouille C, Guidi-Guilvard LD, Ezat U (1997) Drastic changes in deep-sea sediment porewater
620   composition induced by episodic input of organic matter. Limnol Oceanogr 42: 980-986

621   Glud RN (2008) Oxygen dynamics of marine sediments. Marine Biology Research 4(4): 243-289

622

623   Grasshoff K, Ehrhardt M, Kremling K (1983) Methods of Seawater Analysis, second, revised and extended
624   edition. Verlag Chemie, Weinheim, Germany, 420 pp

625

626   Grenz C, Cloern JE, Hager SW, Cole BE (2000) Dynamics of nutrient cycling and related benthic nutrient and
627   oxygen fluxes during a spring phytoplankton bloom in South San Francisco Bay (USA). Marine Ecology
628   Progress Series 197: 67-80

629   Hall. PDJ, Anderson. LG, Rutger van der, Loeff. MM, Snudby B, Vesterlund. SFG (1989) Oxygen uptake
630   kinetics in the benthic boundary layer. Limnol. Oceanogr. 34: 734-746

631

632   Hammond DE, Fuller C, Harmon D, Hartman B, Korosec M, Miller LG, Rea R, Warren S, Berelson W, Hager
633   SW (1985) Benthic fluxes in San Francisco Bay. Hydrobiologia 129(1): 69-90

634   Hellings L,Dehairs F, Tackx M, Keppens E, Baeyens W (1999) Origin and fate of organic carbon in the
635   freshwater part of the Scheldt Estuary as traced by the stable carbon isotope composition. Biogeochemistry 47:
636   167-186

637   Huettel M, Røy H, Precht E, Ehrenhauss S (2003) Hydrodynamical impact on biogeochemical processes in
638   aquatic sediments. Hydrobiologia 494: 231–236

639

640   Lansard B, Rabouille C, Denis L, Grenz C (2009) Benthic remineralization at the land-ocean interface: A case

641   study of the Rhone River (NW Mediterranean Sea). Estuarine, Coastal and Shelf Science 81(4): 544-554

642   Laruelle GG et al (2009) Anthropogenic perturbations of the silicon cycle at the global scale: the 1 key role of

643   the land-ocean transition. Global Biogeochem. Cy 23, GB4031, 17 PP. doi:10.1029/2008GB003267

644

645   Le Pape O, Del Amo Y, Menesguen A, Arninot A, Quegulner B, Treguer P (1996) Resistance of a coastal

646   ecosystem to Increasing eutrophlc conditions: the Bay of Brest (France), a semi-enclosed zone of western

647   Europe. Cont Shelf Res 16(15):1885-1907

648

649   Meiggs D, Taillefert M (2011) The effect of riverine discharge on biogeochemical processes in estuarine

650   sediments. Limnology and Oceanography 56: 1797-1810

651

652   Michaud E, Desrosiers G, Mermillod-Blondin F, Sundby B, Stora G (2005) The functional group approach to

653   bioturbation: The effects of biodiffusers and gallery-diffusers of the Macomabalthica community on sediment

654   oxygen uptake. Journal of Experimental Marine Biology and Ecology 326(1): 77-88

655

656   Middelburg JJ, Klaver G, Nieuwenhuize J, Vlug T (1995) Carbon and nitrogen cycling in intertidal sediments

657   near Doel, Scheldt estuary. Hydrobiologia 311: 57-69

658

659   Mouret A, Anschutz P, Lecroart P, Chaillou G, Hyacinthe C, Deborde J, Jorissen FJ, Deflandre B, Schmidt S,

660   Jouanneau JM (2009) Benthic geochemistry of manganese in the Bay of Biscay, and sediment mass

661   accumulation rate. Geo-Marine Letters 29: 133-149

662

663   Mügler C, Rabouille C, Bombled B, Montarnal P (2012) Impact of spatial heterogeneities on oxygen

664   consumption in sediments: Experimental observations and 2D numericalmodeling. Journal of Geochemical

665   Exploration 112: 76-83

666

667   Nixon SW et al (1996) The fate of nitrogen and phosphorus at the land–sea margin of the North Atlantic Ocean.

668   Biogeochemistry 35: 141–180

669

670   Pastor L, Cathalot C, Deflandre B, Viollier E, Soetaert K, Meysman FJR, Ulses C, Metzger E, Rabouille C

671   (2011a) Modeling biogeochemical processes in sediments from the Rhône River prodelta area (NW

672   MediterraneanSea). Biogeosciences 8: 1351–1366

673

674   Pastor L et al (2011b) Influence of the organic matter composition on benthic oxygen demand in the Rhône

675   River prodelta (NW MediterraneanSea). Continental Shelf Research 31(9): 1008-1019

676

677 Rabouille C, Gaillard JF (1994). Simulation of the sediment behavior during a benthic chamber deployment on
678   the deep-sea floor. Oceanologia Acta 17: 405-416

679

680 Rabouille C, Mackenzie F, Ver LM (2001) Influence of the human perturbation on carbon, nitrogen and oxygen
681   biogeochemical cycles in the global coastal ocean. Geochim Cosmochim Acta *65*: 3615-3639

682

683 Rabouille C, Denis L, Dedieu K, Stora G, Lansard B, Grenz C (2003) Oxygen demand in coastal marine
684 sediments: comparing in situ microelectrodes and laboratory core incubations. Journal of Experimental Marine
685 Biology and Ecology 285-286: 49-69

686

687 Ragueneau O, Chauvaud L, Leynaert A, Thouzeau G, Paulet YM, Bonnet S, Lorrain A, Corvaisier R, Le Hir M,

688 Jean F, J. Clavier (2002) Direct evidence of a biologically active coastal silicate pump: ecological implications.

689 Limnology Oceanography 47:1849-1854

690

691 Raimonet M (2011) Cycle benthique du silicium dans les estuaires: observations et modélisation à différentes

692 échelles spatio-temporelles. Ph D thesis, Université de Bretagne Occidentale, Brest, pp 179

693

694 Raimonet M, Andrieux-Loyer F, Ragueneau O, Michaud E, Kerouel R, Philippon X, Nonent M, Mémery L (in

695 review) Strong gradient of benthic biogeochemical processes along a macrotidal temperate estuary: focus on P

696 and Si cycles. Biogeochemistry

697

698 Resing JA, Mottl MJ (1992) Determination of manganese in seawater using flow injection analysis with on-line

699 preconcentration and spectrophotometric detection. Anal. Chem. 64(22): 2682–2687

700

701 Revsbech NP, Jorgensen BB (1986) Microelectrodes: their use in microbial ecology. Adv Microb Ecol 9: 293-
702   352

703

704 Revsbech NP (1989) An oxygen microsensor with a guard cathode. Limnol Oceanogr 34: 474-478

705

706 Ruiz-Fernández AC, Hillaire-Marcel C, Ghaleb B, Soto-Jiménez M, Páez-Osuna, F (2002) Recent sedimentary
707   history of anthropogenic impacts on the Culiacan River Estuary, northwestern Mexico: geochemical
708   evidence from organic matter and nutrients. Environ. Pollut. 118: 365–377

709

710 Sarradin PM, Le Bris N, Le Gall C, Rodier P (2005) Fe analysis by the ferrozine method: Adaptation to fia
711   towards in situ analysis in hydrothermal environment. Talanta 66(5):1131–1138

23

712

713 Seeberg-Elverfeldt J, Schlüter M, Feseker Tomas, Kölling M (2005) Rhizon sampling of porewaters near the
714 sediment-water interface of aquatic systems. Limnol Oceanogr: Methods 3: 361–371

715

716 Seitzinger SP (1988) Denitrification in freshwater and coastal marine ecosystem: ecological and geochemical
717 significance. Limnol. Oceanogr. 33: 702-724

718

719 Sweerts JP, De Beer D (1989) Microelectrode measurements of nitrate gradients in the littoral and profundal
720 sediments of a meso-eutrophic lake (lake Vechten, the Netherlands). App Envir Microb 55: 754-757

721

722 Tabatabai MA (1974) A rapid method for determination of sulphate in water samples. Environmental Letters
723 7(3): 237-242

724

725 Tesi T, Miserocchi S, Goni MA, Langone L, Boldrin A, Turchetto M (2007) Organic matter origin and
726 distribution in suspended particulate materials and surficial sediments from the western Adriatic Sea (Italy).
727 Estuar. Coast. Shelf S 73: 431–446

728

729 Thamdrup B, Wurgler Hansen J, Barker Jorgensen B (1998) Temperature dependance of aerobic respiration in a
730 costal sediment. FEMS Microiology Ecology 25: 189-200

731

732 Thouzeau G, Grall J, Clavier J., Chauvaud L, Jean F, Leynaert A, Ni Longphuirt S, Amice E, Amouroux D
733 (2007) Spatial and temporal variability of benthic biogeochemical fluxes associated with macrophytic and
734 macrofaunal distributions in the Thau lagoon (France). Estuarine, Coastal and Shelf Science 72(3): 432-446

735

736 Xiao HY, Liu CQ (2010) Identifying organic matter provenance in sediments using isotopic ratios in an urban
737 river. Geochem J 44:181-187

Tables

Table 1 Environmental parameters (temperature T (°C), salinity S, depth D (m), river discharge Q (m^3 s^{-1}), and bottom water O_2 concentration O_{2bw} (µM)) at each station and season during benthic sampling

Station	T (°C)	S	D (m)	Q (m3 s-1)	O_{2bw} (µM)
February					
E1	8	0	1	18.5	377
E2	7.6	17.5	2	15.7	310
E3	8.2	29	3.5	14.5	297
A1	7.7	0	2.5	64.6	415
A2	7.4	13.7	3	54.1	352
A3	8	20	1.75	49.7	293
May					
E1	12.3	0	1	4.69	330
E2	13.4	21.7	1.5	4.33	273
E3	12.8	33.5	6	4.24	277
A1	14.4	0	2	10.4	314
A2	14	22.5	3	9.95	277
A3	13.5	24.6	2	10.7	282
July					
E1	16.7	0	0.5	2.79	304
E2	16.7	12.2	1	2.48	213
E3	17.7	33.5	6	1.77	225
A1	19.7	0	0.5	4.24	292
A2	19.5	27.5	1.5	5.01	202
A3	19.1	30.9	3	3.59	345
October					
E1	15	0.8	0.5	1.45	294
E2	15.1	29.6	1.2	1.45	204
E3	15.3	34.2	8	1.42	217
A1	14.2	8.7	1	3.67	278
A2	15.5	29.9	1	3.47	225
A3	15	33	2.5	4.91	228

Figures
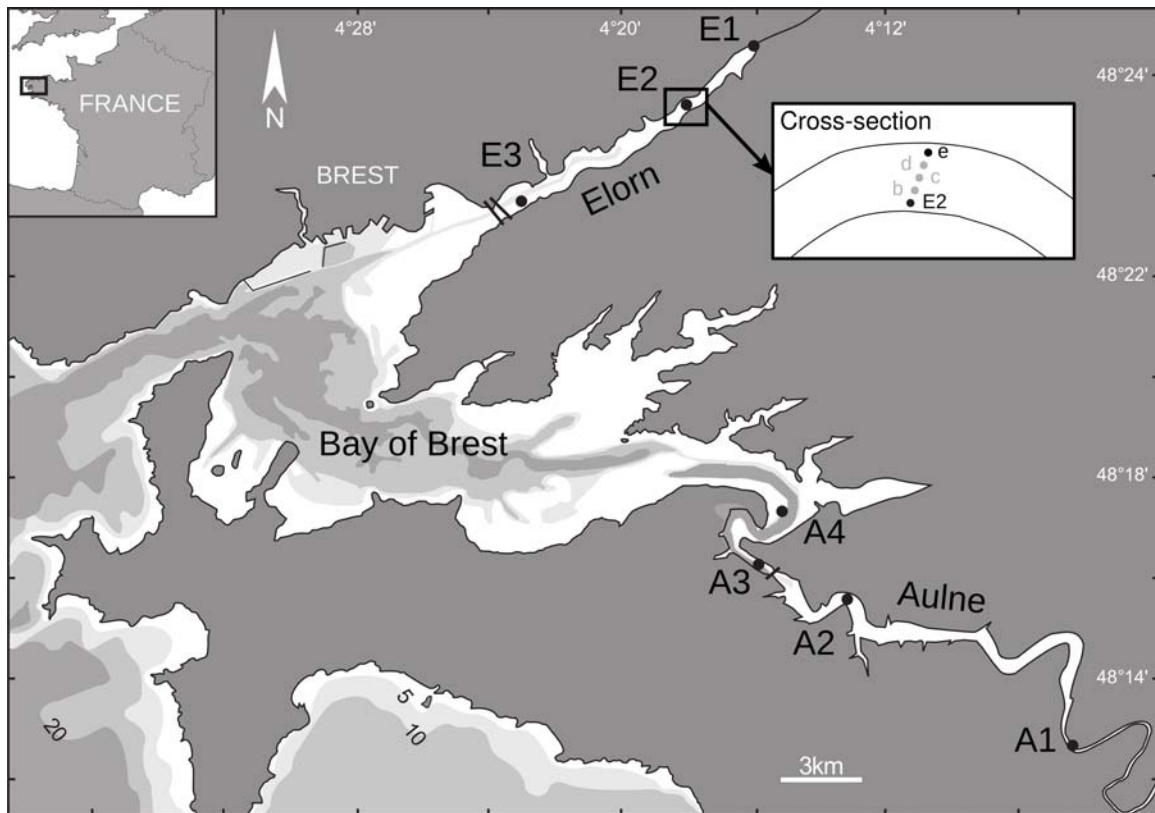
Fig.1 Study area and location of stations sampled in February, May, July and October 2009 along the Elorn and Aulne estuaries
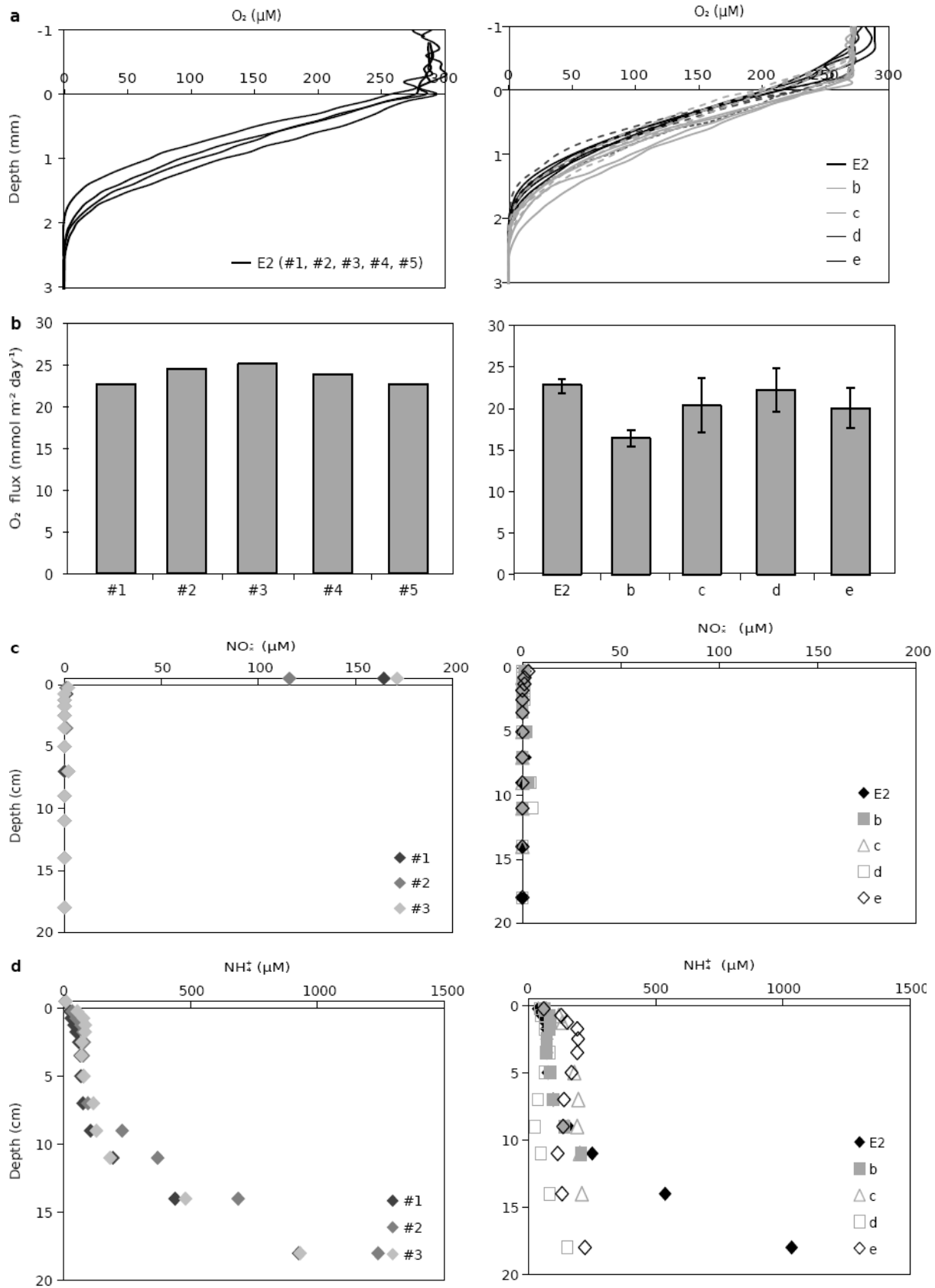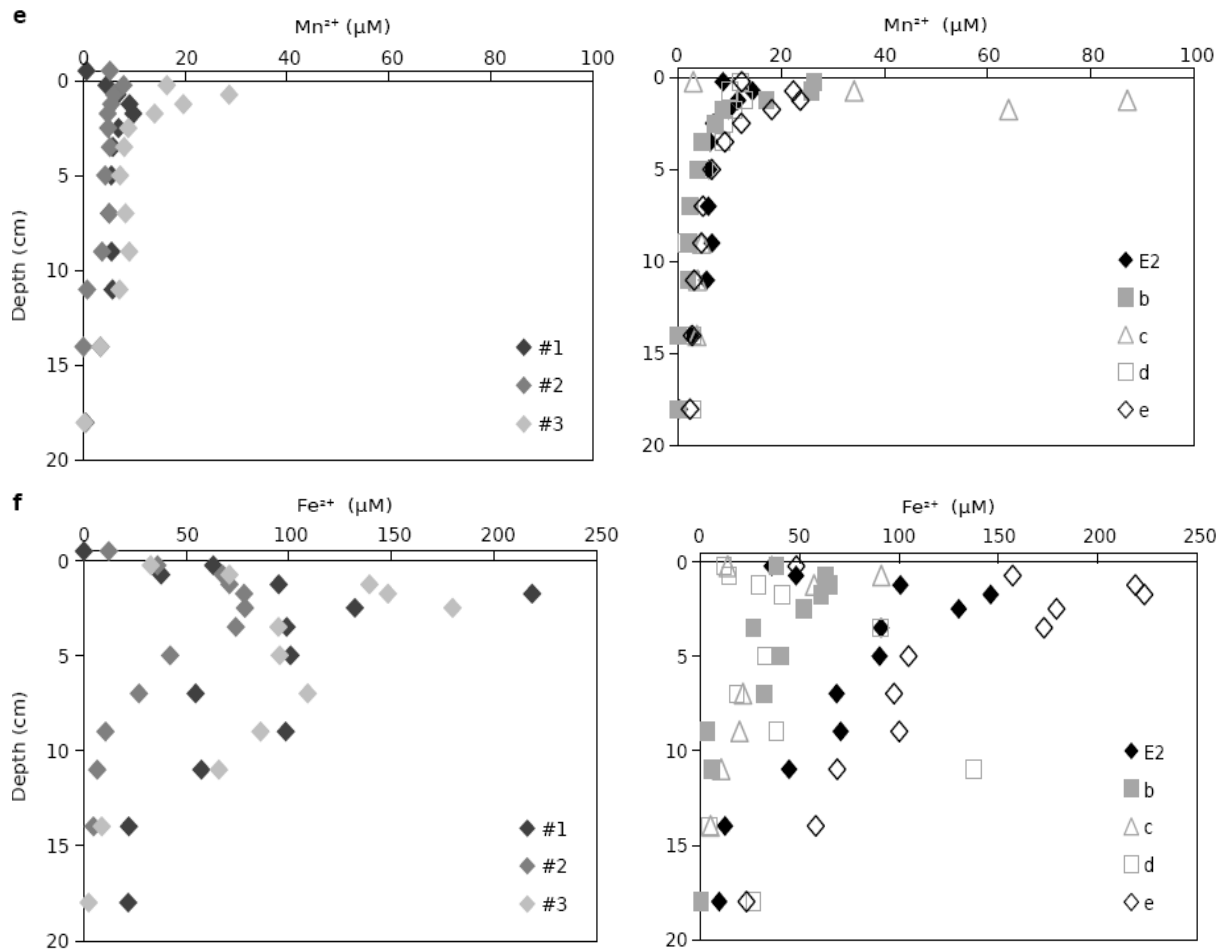
Fig.2 O_2 concentrations (a), O_2 fluxes (b), NO_x^- (c), NH_4^+ (d), Fe^{2+} (e), and Mn^{2+} concentrations (f) in pore waters at station E2 (left panels) and in a transversal cross-estuarine section (right panels) in May 2009
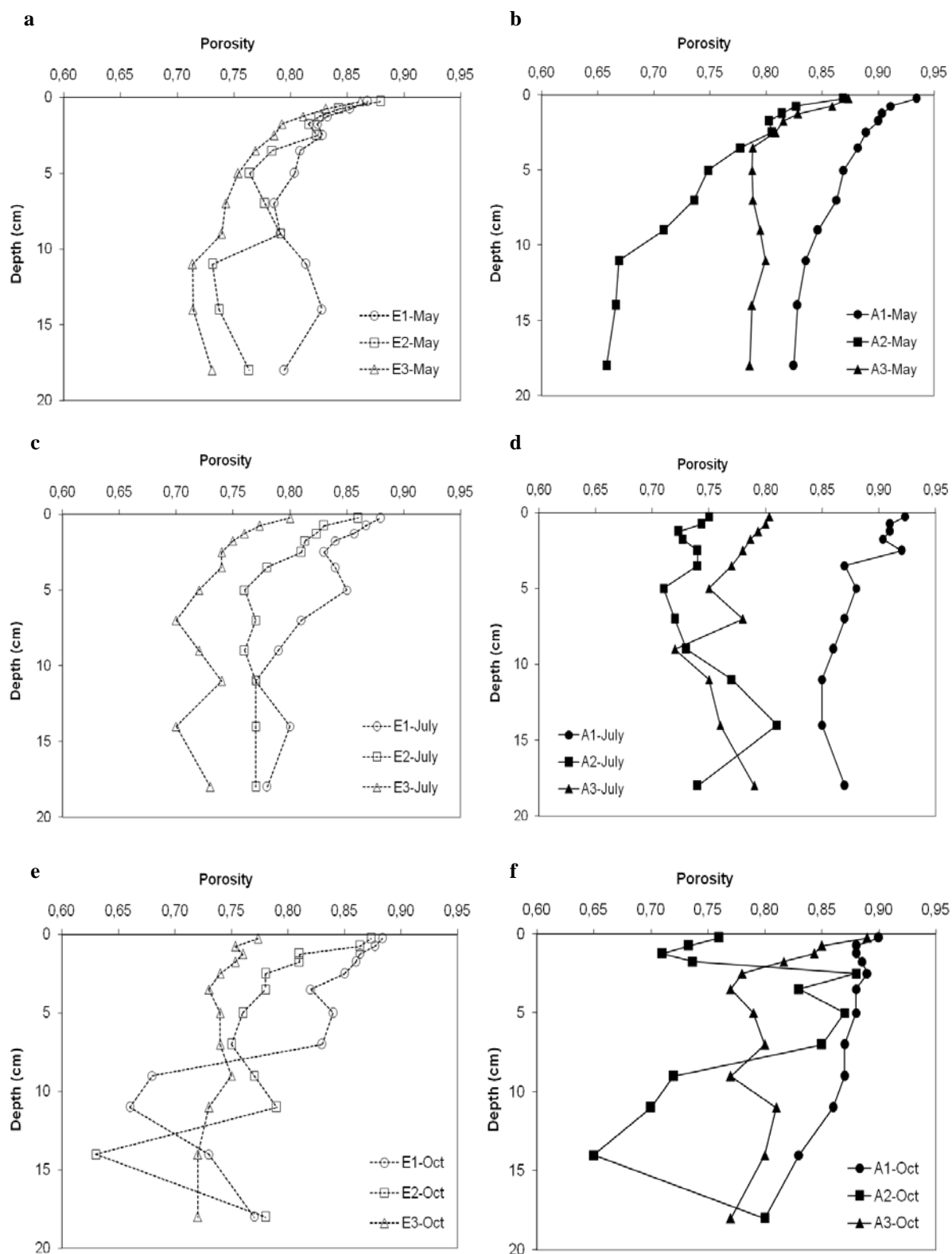
Fig.3 Porosity profiles over depth in May (a, b); in July (c, d) and in October (e, f). Left and right panels represent the Elorn and Aulne Estuary, respectively
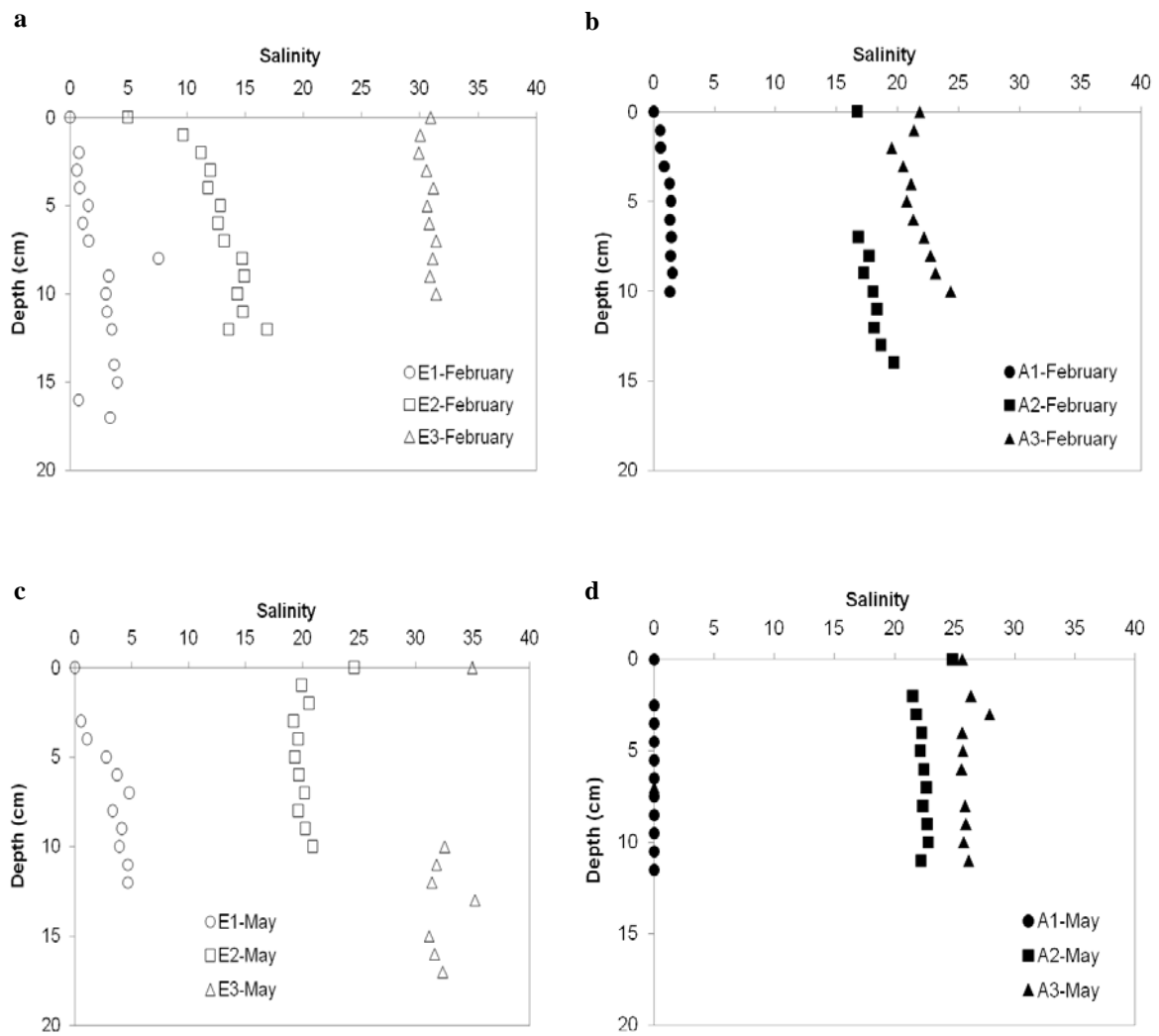
Fig.4 Salinity profiles over depth in February (a, b); in May (c, d). Left and right panels represent the Elorn and Aulne Estuary, respectively.
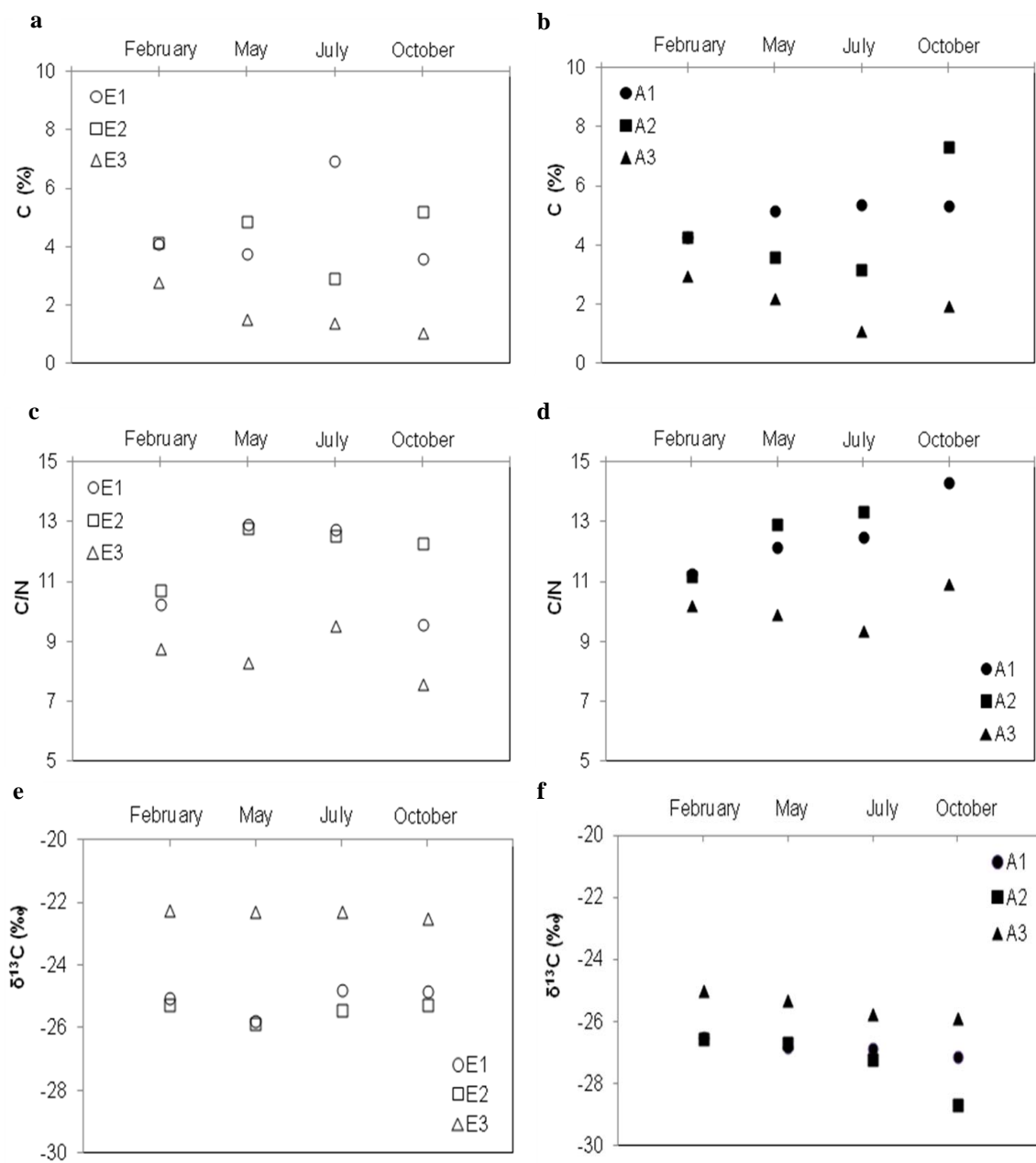
Fig.5 Organic carbon contents (a) and (b), Carbon to Nitrogen atomic ratio (c) and (d), isotopic of carbon (e) and (f) measured on the top layer for Elorn and Aulne Estuary respectively, on level 0-0.5 cm in February and on 50/50 mix of level 0-0.5 and 2-3 cm in other cruises May, July and October
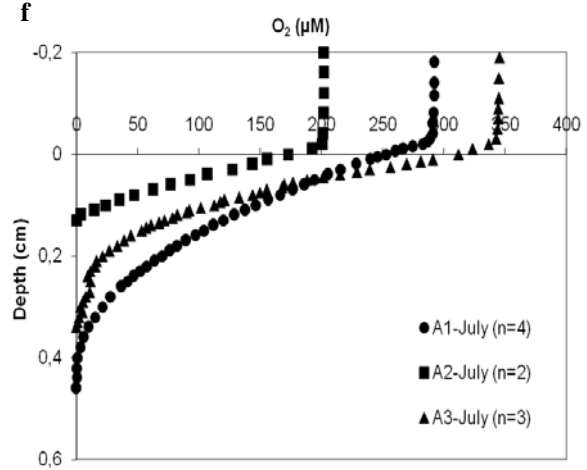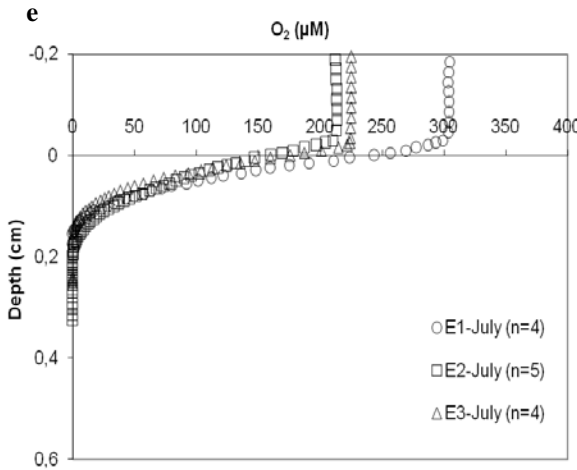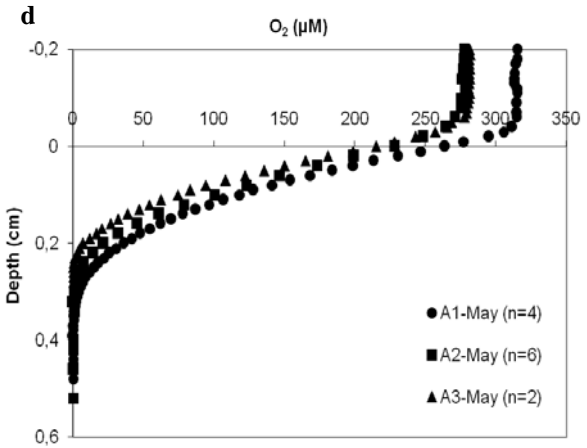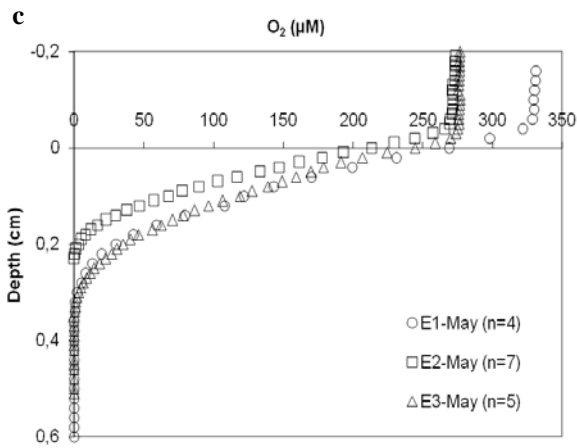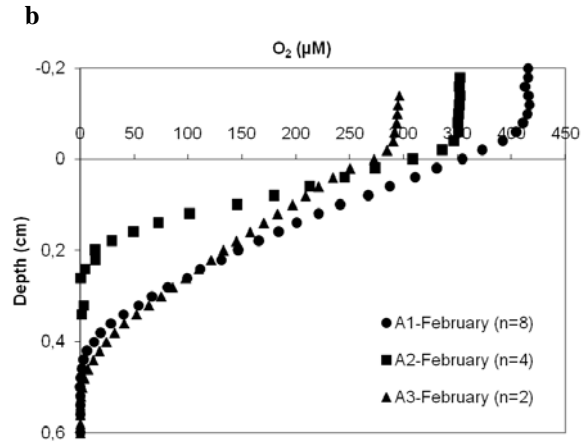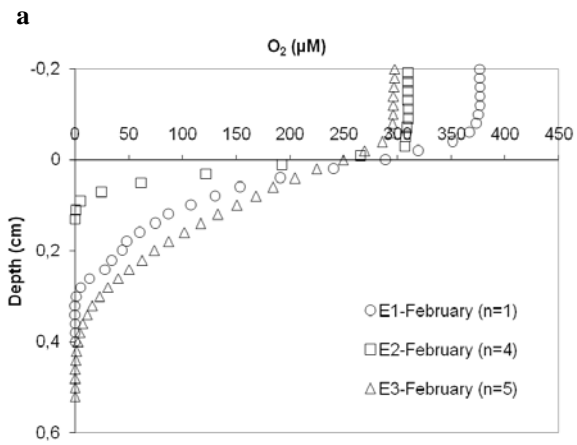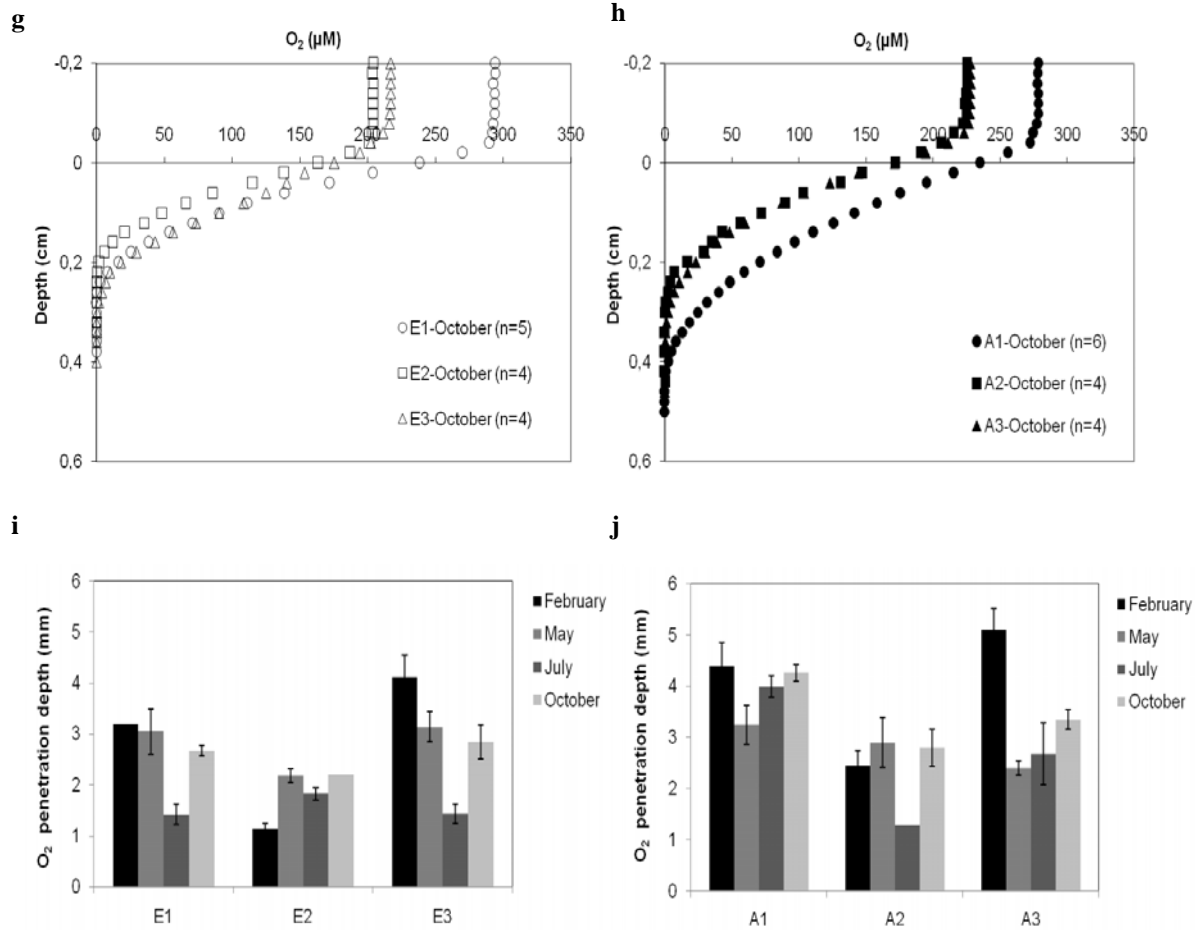
Fig.6 Average oxygen profiles over depth in February (a, b); in May (c, d); in July (e, f) and in October (g, h); oxygen penetration depth at all seasons February, May, July and October (i, j). Left and right panels represent the Elorn and Aulne Estuary, respectively
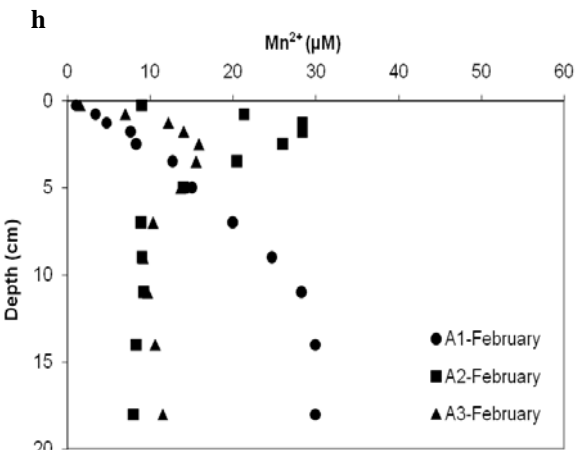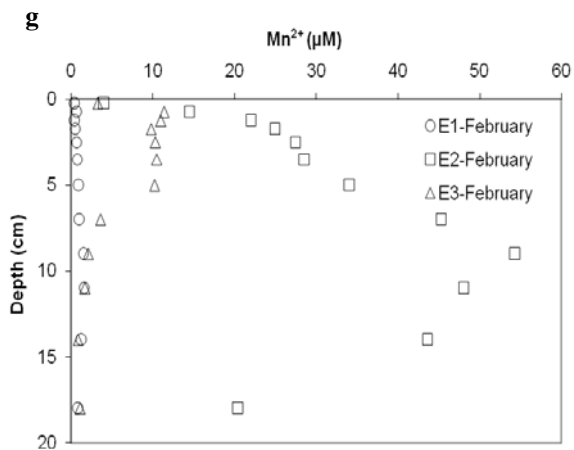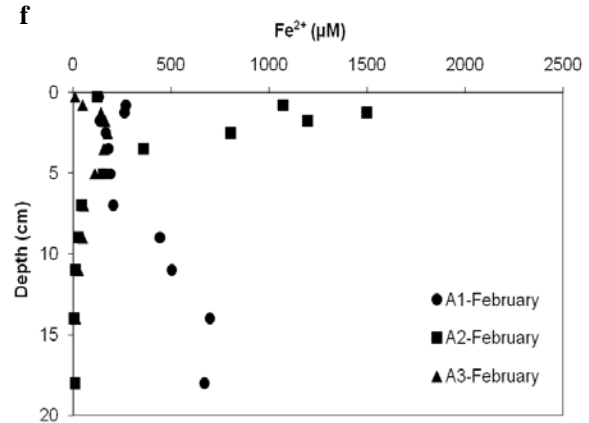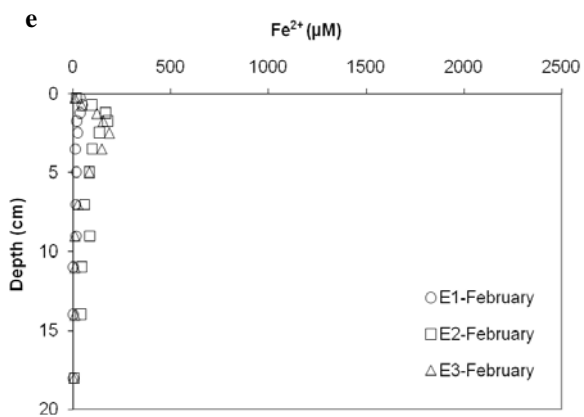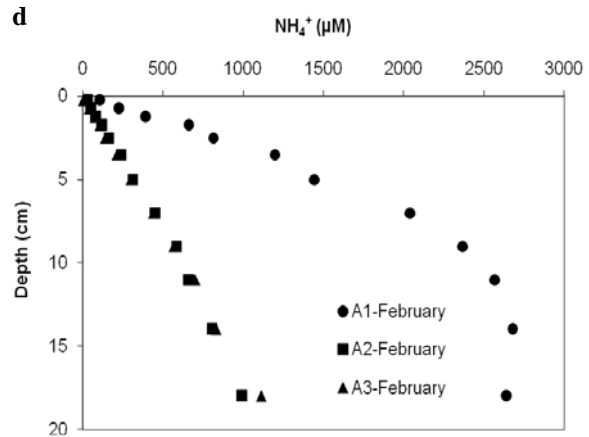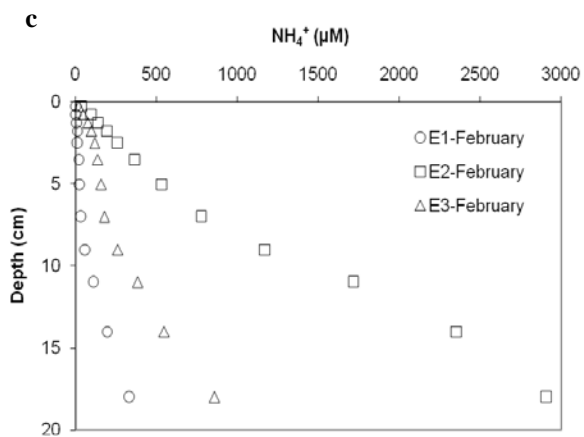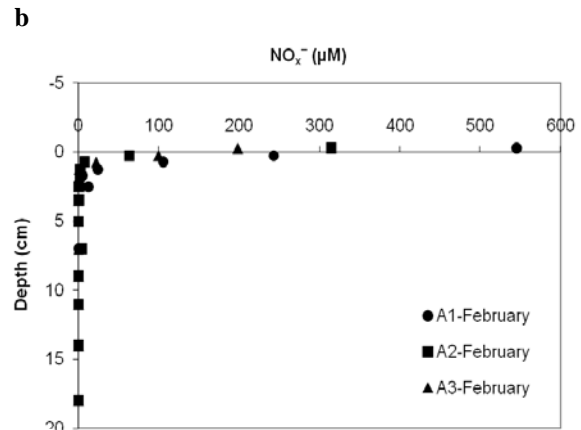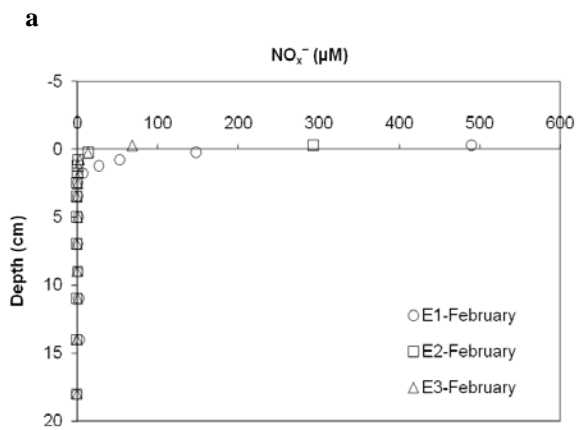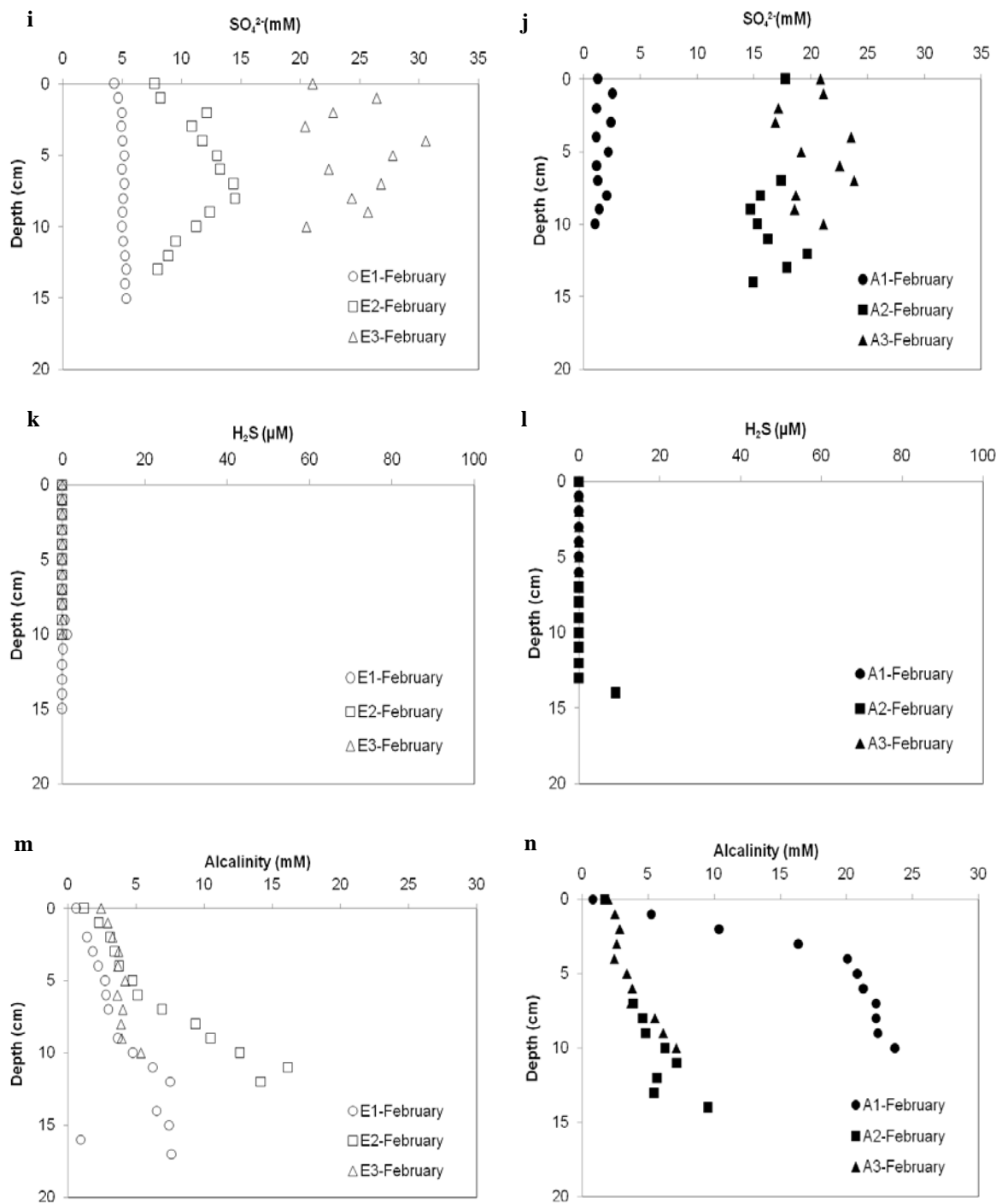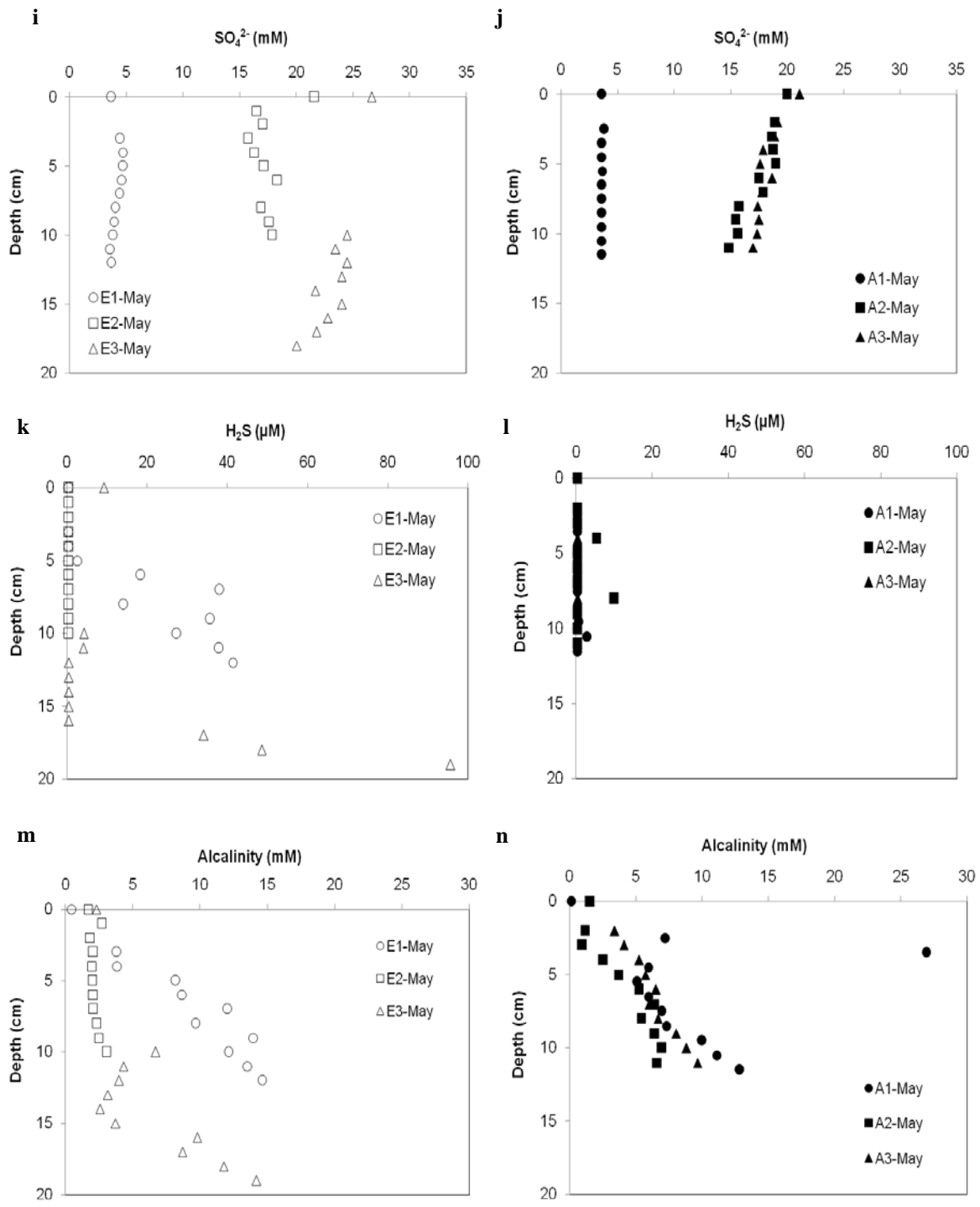
Fig.7 Nitrogen profiles over depth (a, b), ammonium profiles over depth (c, d), iron profiles over depth (e, f), manganese profiles over depth (g, h), sulfate profiles over depth (i, j), sulfide profiles over depth (k, l), alcalinity profiles over depth (m, n). Left and right panels represent the Elorn and Aulne Estuary, respectively, in February
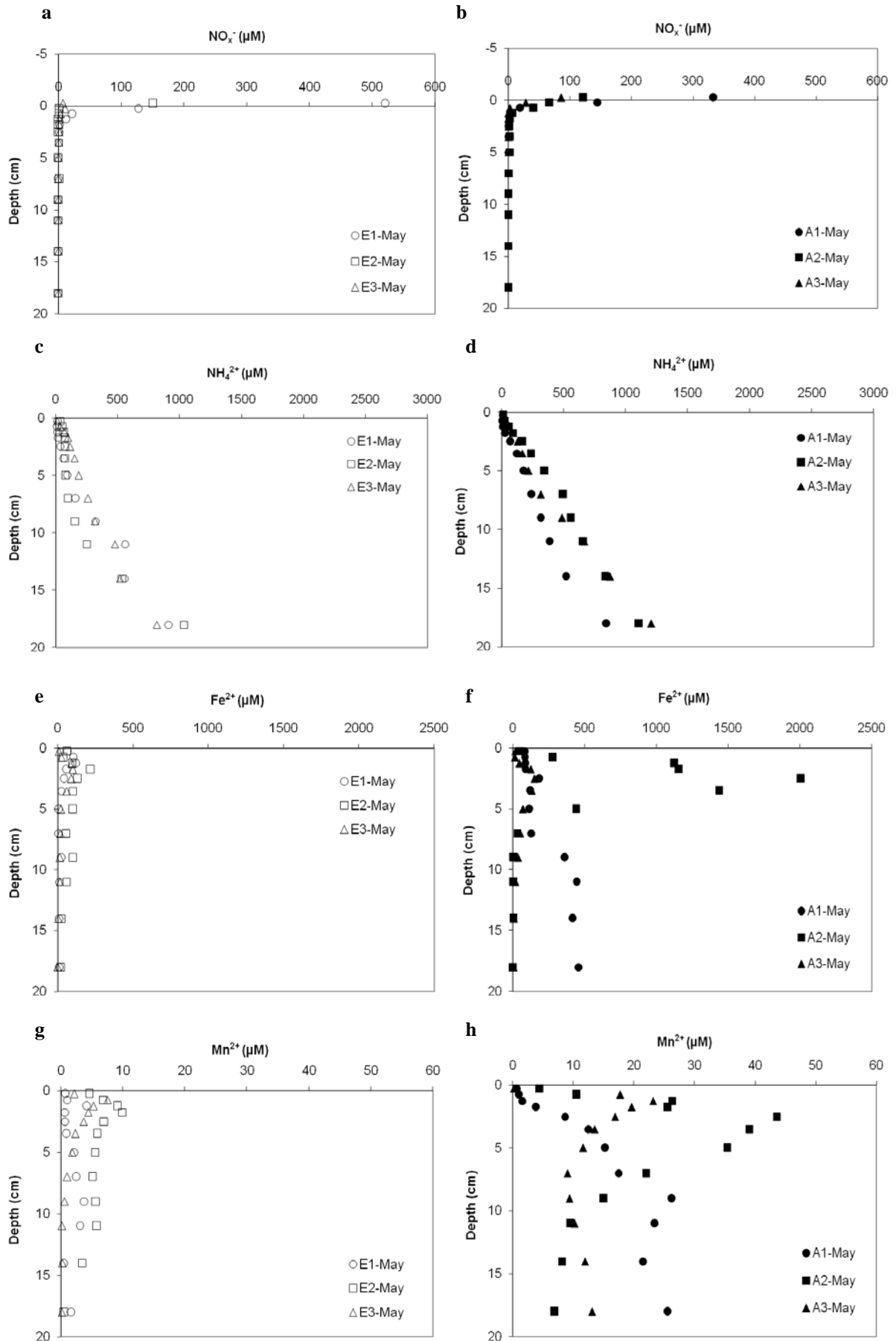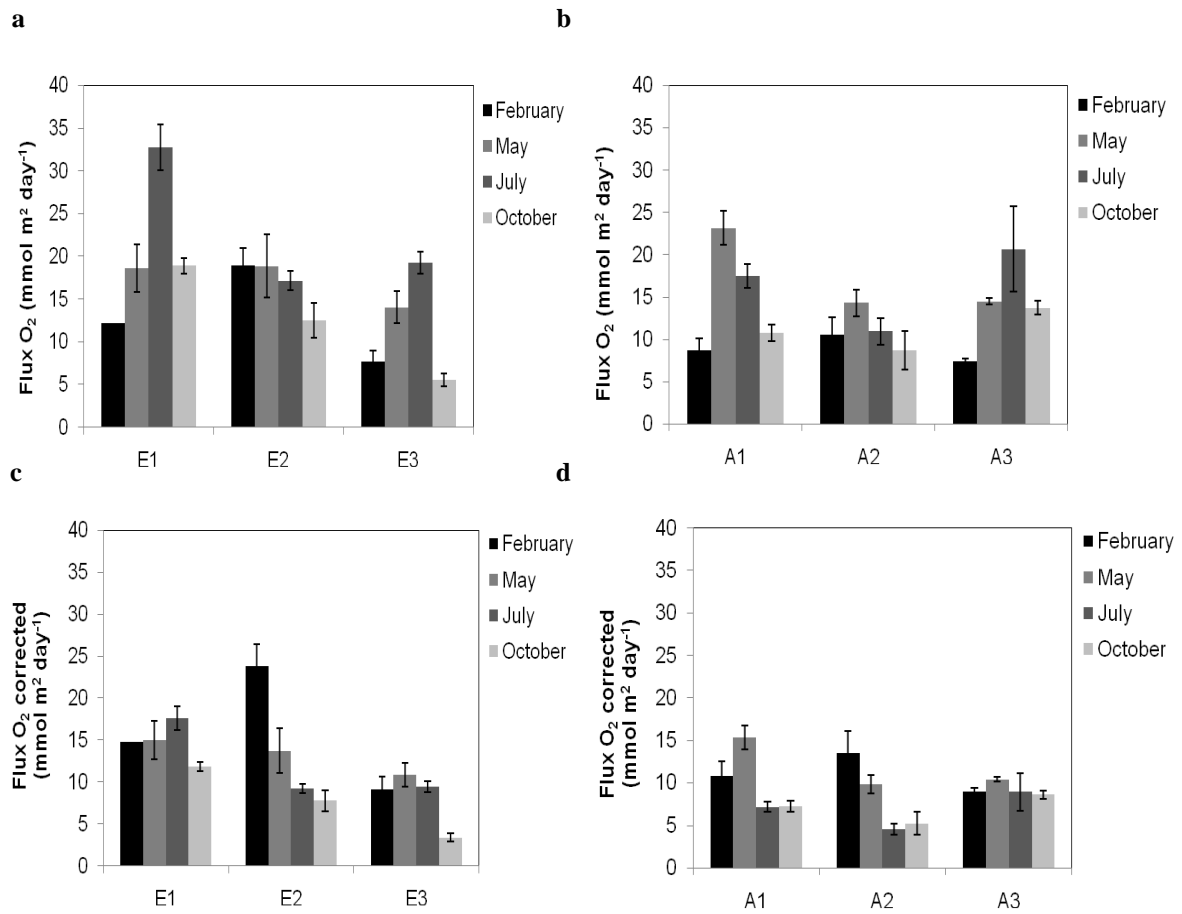
Fig.8 Nitrate profiles over depth (a, b), ammonium profiles over depth (c, d), iron profiles over depth (e, f), manganese profiles over depth (g, h), sulfate profiles over depth (i, j), sulfide profiles over depth (k, l), alcalinity profiles over depth (m, n). Left and right panels represent the Elorn and Aulne Estuary, respectively, in May

Fig.9 Diffusive oxygen fluxes at February, May, July and October (a, b). Diffusive oxygen fluxes recalculated for a temperature of 10°C corresponding to each season February, May, July and October (c, d). Left and right panels represent the Elorn and Aulne Estuary, respectively
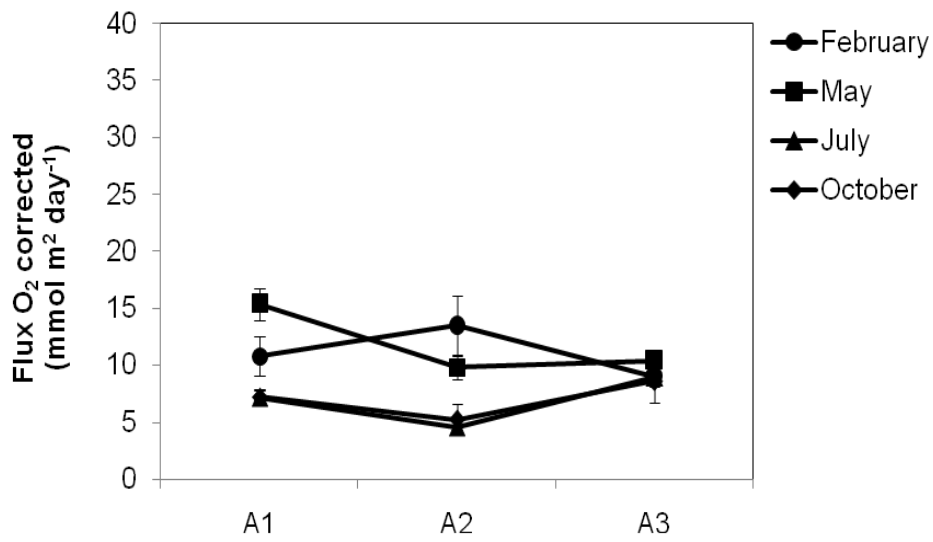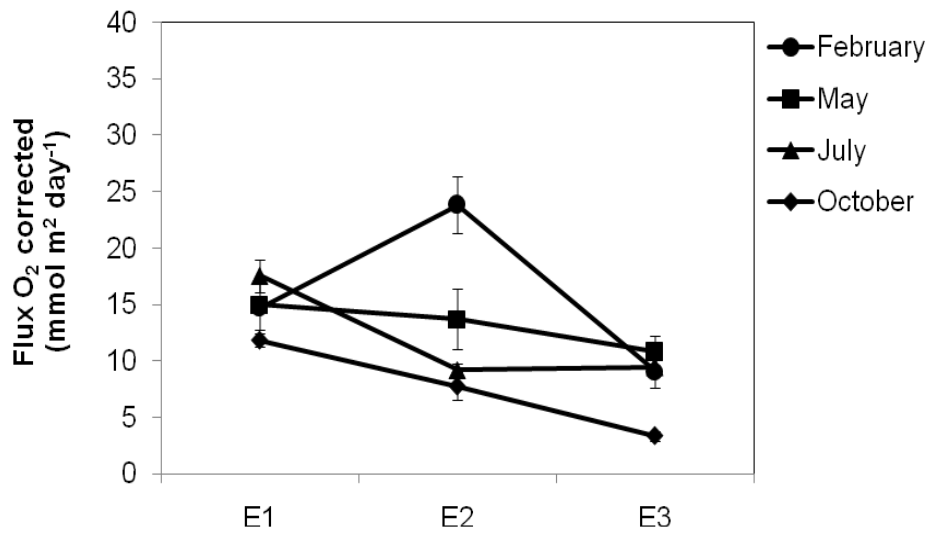
Fig.10: T-corrected diffusive oxygen fluxes (at 10°C) along the Elorn and Aulne estuaries at the four different seasons
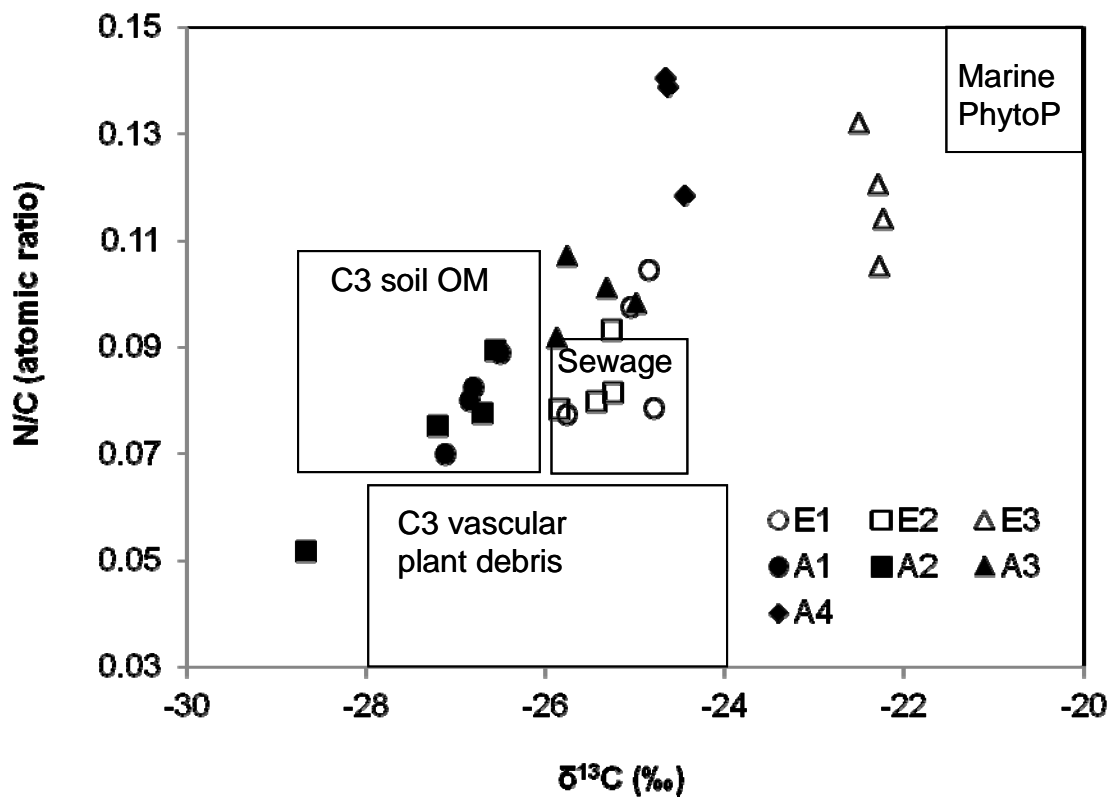
Fig.11 Stable isotopic composition of organic carbon ($\delta^{13}C$) versus atomic nitrogen:carbon ratios (N/C) measured in the top sediment layer for Elorn and Aulne Estuary respectively, on level 0-0.5 cm in February cruise and on 50/50 mix of level 0-0.5 and 2-3 cm in May, July and October. The compositions of four possible organic carbon sources (terrigenous C3 vascular plant, C3 soil OM, sewage and marine phytoplankton) are also plotted to illustrate the relative influence of each source. Station A4 is located in the outer estuary downstream of A3, with larger salinity waters